General Disclaimer

One or more of the Following Statements may affect this Document

- This document has been reproduced from the best copy furnished by the organizational source. It is being released in the interest of making available as much information as possible.

- This document may contain data, which exceeds the sheet parameters. It was furnished in this condition by the organizational source and is the best copy available.

- This document may contain tone-on-tone or color graphs, charts and/or pictures, which have been reproduced in black and white.

- This document is paginated as submitted by the original source.

- Portions of this document are not fully legible due to the historical nature of some of the material. However, it is the best reproduction available from the original submission.

CR 137584

MCR-74-372
NAS2-7489

Part II

Final
Report

October 1974

Evaluation of Fluid
Behavior in Spinning
Toroidal Tanks

A Feasibility Study
of Developing
Toroidal Tanks
for a Spinning
Spacecraft

MARTIN MARIETTA

MCR-74-372
NAS2-7489

PART II   FINAL
REPORT   OCTOBER 1974

EVALUATION OF FLUID
BEHAVIOR IN SPINNING
TOROIDAL TANKS

A FEASIBILITY STUDY OF
DEVELOPING TOROIDAL TANKS
FOR A SPINNING SPACECRAFT

APPROVED

DALE A. FESTER
PROGRAM MANAGER

PREPARED BY

JOHN E. ANDERSON

PREPARED FOR

NATIONAL AERONAUTICS AND SPACE
ADMINISTRATION
AMES RESEARCH CENTER
MOFFETT FIELD, CALIFORNIA

PREPARED BY

MARTIN MARIETTA CORPORATION
DENVER DIVISION
DENVER, COLORADO 80201

FOREWORD _

CONTENTS

FIGURE

SUMMARY

An experimental program was conducted for the purpose of evaluating propellant behavior characteristics in spinning toroidal tanks that could conceivably be used in a retro-propulsion system for a proposed outer-planet Pioneer orbiter. The effects of typical mission requirements and related phenomena upon propellant slosh and settling and orientation and stability of the ullage were investigated in a subscale model tank under both one-g and low-g acceleration environments. Specific conditions included in the study were axial acceleration, spin rate, spin-rate change, and spacecraft wobble, both singly and in combination. A one-eighth scale, transparent tank was used for testing. A simulated propellant acquisition device was included in the tank. The low-g testing was accomplished in the Martin Marietta 2.1-second drop tower facility. Fluid behavior was recorded with a high-speed movie camera. Liquid loadings in the test tank ranged from 5% to 96% full.

Methanol and water in combination with appropriate spin-rates and accelerations of the scale model system were used to simulate the behavior of fluorine, nitrogen tetroxide, monomethylhydrazine, and hydrazine.

A general conclusion reached from the experimental results was that no major fluid behavior problems would be encountered with the use of toroidal tanks containing any of the four propellants in a proposed spin-stabilized orbiter spacecraft. In the absence of perturbing forces during coast phases, the propellant distribution would be uniform with a stable and symmetrical ullage volume at all propellant loadings. Test results indicated that slosh problems during liquid settling following engine ignition would be minor, since the propellant acquisition device provided adequate damping for liquid volumes of 25% or less and helped to damp sloshing at large propellant loadings. Some additional baffling could easily be installed with little weight penalty if more rapid damping is desired for liquid volumes greater than 25%. Additional testing is necessary to determine the magnitude of slosh forces and frequencies in a spinning torus.

The most severe fluid behavior problems observed resulted from simulated spacecraft wobble which produced an unsymmetrical propellant distribution. However, this problem is not considered serious, since the design of the proposed spin-stabilized spacecraft includes a dynamic damper to reduce wobble to zero once the cause of the wobble (e.g., misaligned thrust during engine

operation) disappears. Depending on the frequency of the propellant motion in the spinning toroidal tanks, some dynamic damping of the wobble might also be furnished by the propellants. Additional testing in this area would be desirable.

Test results indicated that spacecraft spin-rate changes would not cause major effects on spacecraft operation, propellant acquisition, or tank design.

In 1973, a study was initiated to investigate the feasibility
of developing a toroidal tank system for use in a spin-stabilized
Pioneer-type orbiter for outer planet missions. The results of
this study (Ref. 1) indicated that toroidal tanks employing sur-
face tension propellant management devices could be fabricated
and employed in the spinning spacecraft with no major problems
or difficulties. Another study conducted by TRW Systems (Ref. 2)
indicated certain advantages in weight, packaging, and structural
mounting if two toroidal tanks were to be used in the spinning
spacecraft rather than combinations of two or four spherical
tanks. However, the results of these studies were analytical
i.. nature and lacked experimental confirmation in many respects.
One of the major areas of concern was the fluid behavior character-
istics associated with a spinning toroidal tank. Before consider-
ing a full-size tank development program, it was believed useful
to conduct scale model testing to assess the nature of propellant
slosh and settling and of ullage orientation and stability
characteristics of propellants contained in a spinning toroidal
tank. The effects of axial acceleration, spin rate, spin rate
changes, and spacecraft wobble singly and in combination on fluid
behavior for propellant loadings from nearly full to nearly empty
were of interest.

The present study was carried out in four consecutive steps to
evaluate fluid behavior in spinning toroidal tanks. The four
steps were: Test Planning, Test Hardware Design and Assembly,
Testing, and Documentation. The program schedule, based on a
March 18, 1974 starting date, is shown in Figure 1.

Major program guidelines and constraints were specified as follows.
First, testing should be conducted in a subscale, transparent tank
in order to observe and re.ord the fluid behavior photographi-
cally. The tank was to contain a simulated propellant management
device. Propellants to be considered for simulation in test were
nitrogen tetroxide, fluorine, monomethylhydrazine and hydrazine.
Dynamic conditions to be simulated singly and in combination
during the test program were stipulated as follows:

Axial Acceleration	0 to 0.1g
Spin Rate	0 to 20 rpm
Spin Rate Change	1 rpm/sec
Wobble (nutation of spin axis)	1.6° minimum

1974

	MAR	APRIL	MAY	JUNE	JULY	AUGUST	SEPTEMBER	OCTOBER
	18 25	1 8 15 22 29	6 13 20 27	3 10 17 24	1 8 15 22 29	5 12 19 26	2 9 16 23 30	7 14
PROGRAM GO-AHEAD	△							
TEST PLANNING								
TEST HARDWARE DESIGN AND ASSEMBLY								
TESTING								
ULLAGE ORIENTATION								
SETTLING								
WOBBLE EFFECTS								
SPIN RATE CHANGE								
DOCUMENTATION					△			
MID-TERM REVIEW								
FINAL REVIEW							△	
FINAL REPORT								△
DRAFT								
FINAL								

The initial effort was devoted to development of the test plan
to meet the program objectives. In addition to establishing
types of tests and test conditions, it was also necessary to
design test hardware compatible with the limitations imposed by
the test facilities. The same test hardware was to be used in
both bench (one-g) and drop tower (low-g) facilities.

The following sections contain a discussion of the Martin
Marietta Low-G Test Facility (drop tower) and a description of
the test hardware used in this facility.

A.   DROP TOWER FACILITY

The drop tower is located in the Vertical Test Fixture at the
Denver Division of Martin Marietta Corporation. A free-fall
distance of 22.9 meters (75 feet) provides a usable low-g test
time of 1.2 seconds.

The drop system, shown in Figure 2, consists of an outer capsule
(drag shield), and a smaller inner capsule (test cell) that con-
tains the experiment, power supply, and instrumentation. For
zero-g tests, the test cell falls unguided and independent of the
drag shield. Air drag on the test cell and piston effect (caused
by relative travel between the two capsules) are reduced to an
insignificant acceleration level (less than $10^{-5}g$) by evacuating
the drag shield to absolute pressure levels of less than 5 mm
Hg. The relative travel distance between the two capsules per-
mits a free-fall duration for the test cell of 2.1 sec. The
entire capsule assembly is decelerated in a wheat bin. Peak
deceleration is less than 25g and the deceleration time interval
is less than 0.15 second.

To simulate low-g environments, the test cell is accelerated
relative to the drag shield during the drop by a NEG'ATOR*
spring motor assembly and cable arrangement shown in Figure 2.
The motors provide a near-constant force with linear deflection.
The average acceleration applied to the test specimen is cal-
culated by dividing the applied spring force by the test cell
mass.

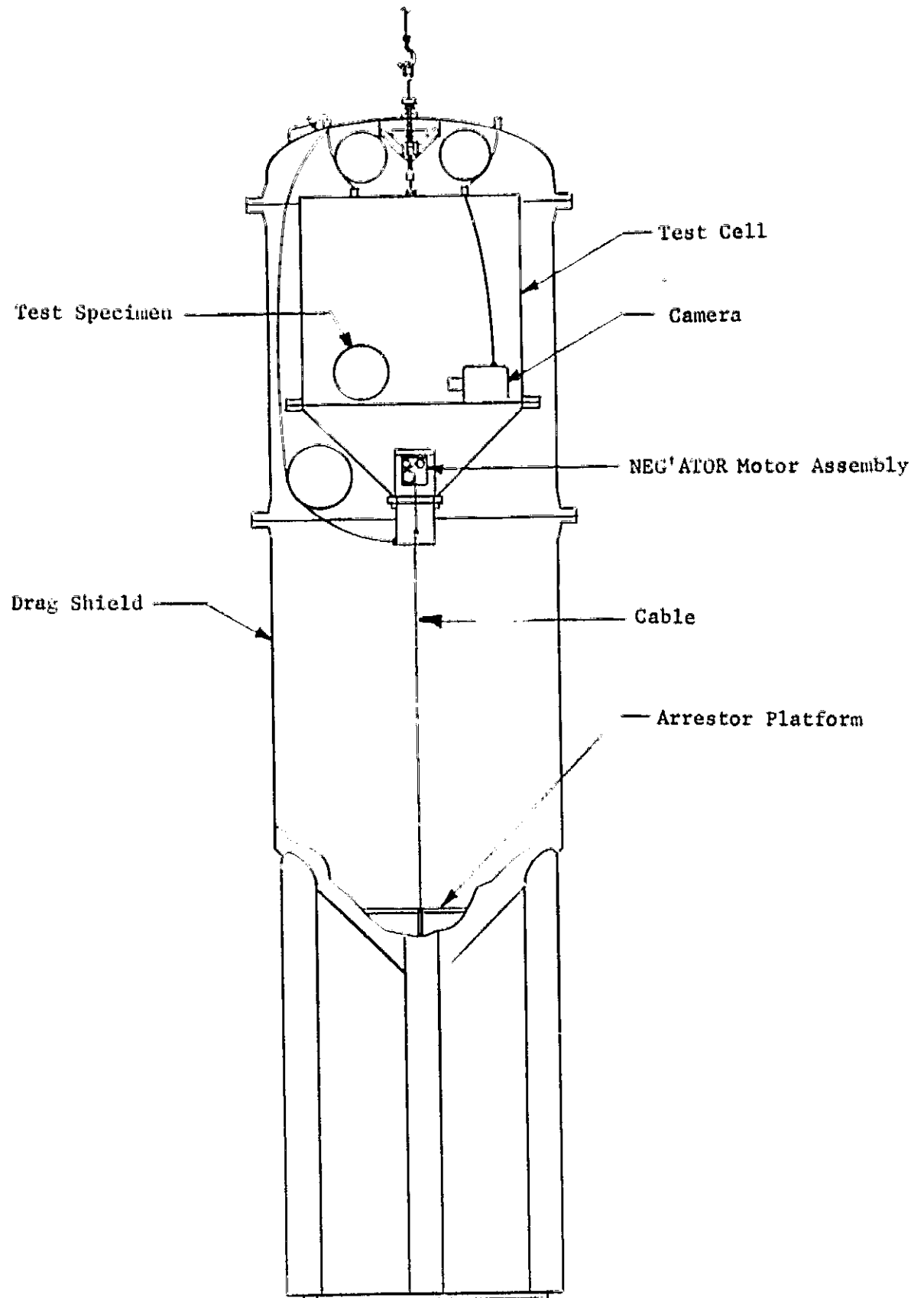*Manufactured by Hunter Spring Company, Hatfield, Pennsylvania

Figure 2: Low-G Drop Capsule Assembly

4

The test cell contains, in addition to the test specimen, a 16-mm Milliken Model DBM3a camera, a battery pack, and light sources for illuminating the specimen. The Milliken camera permits photographic documentation up to 200 frames per second.

B.   TEST HARDWARE DESIGN

Several factors were considered in establishing the size of the toroidal test tank to be used in the drop tower. The first factor was fluid reorientation time, defined as the time for the liquid-gas interface to reach its equilibrium zero-gravity orientation after initiating the drop test. Since the duration of the drop test is only 2.1 seconds, this factor should be no more than a small fraction of one second. Reorientation time is proportional to tank size which, therefore, should be made small.

A second factor influencing tank size selection was the optical characteristics of the tank. Since data is recorded only by photographic means, it is necessary that the tank surfaces offer as clear a view of the contained liquid as possible. Surfaces with large curvature tend to refract and distort images more than do flat surfaces. Smaller tanks, with highly curved surfaces, are not as desirable from an optical standpoint as larger ones.

Another consideration was the actual envelope of the test cell available for the test specimen. This envelope is defined not only by the total volume of the test cell but also by camera requirements such as field of view and lens focal length.

An important consideration in selecting a tank size was the scaling relationship between the model and the full-size tank desired. In the case of a toroidal tank, two dimensions are significant, the major and minor radii. In order to keep the scale-model tank geometrically proportional to the full-size tank, the ratio of major to minor radii was made essentially the same, i.e., 3 to 1.

After evaluation of all the above factors, a minor radius of 1.91 cm (0.75 inch) was selected for the model. The corresponding major radius was 5.72 cm (2.25 inches), resulting in a test tank essentially one-eighth the size of the tank of Reference 1. The selected minor radius provided acceptable optical characteristics for data recording and, together with the major radius, defined a tank size compatible with the test cell envelope. Inasmuch as reorientation time data are not presently available

for toroidal tanks, estimates of reorientation times for a spherical tank of radius 1.91 cm (0.75 inch) and a cylindrical annulus with a gap width of 3.81 cm (1.5 inches) were made from References 3 and 4, to provide values from which such times for the toroidal tank model might be deduced. Calculated reorientation times for the sphere and annulus were 0.22 second and 0.14 second, respectively. It was believed that the reorientation time in the toroidal tank would also be in this range so that the selected minor radius was a reasonable choice.

Methods of fabricating the test tank were also investigated. Two methods considered were hot forming of a plexiglass sheet in a die and casting of polyester resin in a mold. Both methods produce symmetrical halves of the torus which are cemented together to form the complete tank. The latter method was selected because a number of test tanks could be produced rapidly at low cost.

The assembly for supporting and spinning the test tank during both bench and drop tower testing is shown in Figure 3. The toroidal test tank was supported on a shaft over a hole in a housing containing two Sun Gun lamps that illuminate the tank from the underside. A mirror for observing the top of the toroidal tank was mounted above at approximately a 45° angle. Orientation of the mirror made it possible to photograph the front and top view of the tank simultaneously.

Spinning of the tank was provided by a high-speed camera motor through a gear box underneath the lamp housing. Only the gear box base is visible in Figure 3. The motor speed was controlled remotely by a rheostat connected by a landline to the motor. A tachometer sensing switch was also mounted on the gear box underneath the lamp housing and was connected by landline to the tachometer located near the power control rheostat.

The shaft used to support and spin the test tank was a solid, straight rod for all tests except those simulating spacecraft wobble. For the wobble tests, the geometric axis of the test tank was displaced by an angle from the instantaneous spin axis. Two approaches were employed to provide the required minimum displacement of 1.6°. The first employed a solid shaft bent at an angle of 2°, as shown in Figure 4. The bent shaft produced the wobble effect in the toroidal tank during spinning.

The second approach, also shown in Figure 4, used a flexible coupling in the spin shaft with a mechanical stop to limit the

Mirror

Sun Gun Lamp

Test Tank

Sun Gun Lamp

Camera

Tachometer   Gear Box   Drive Motor
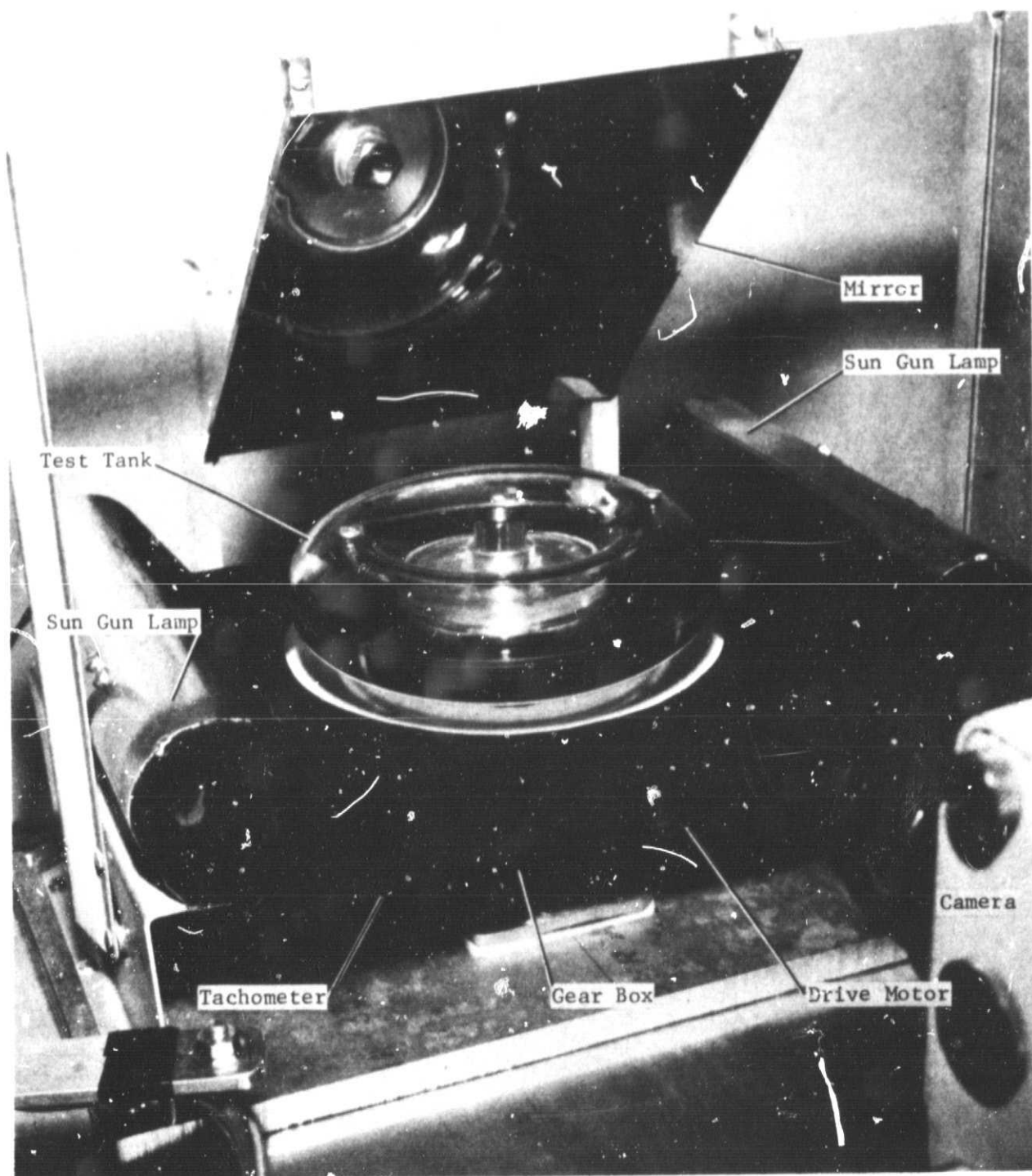
Figure 3   Test Equipment Assembly
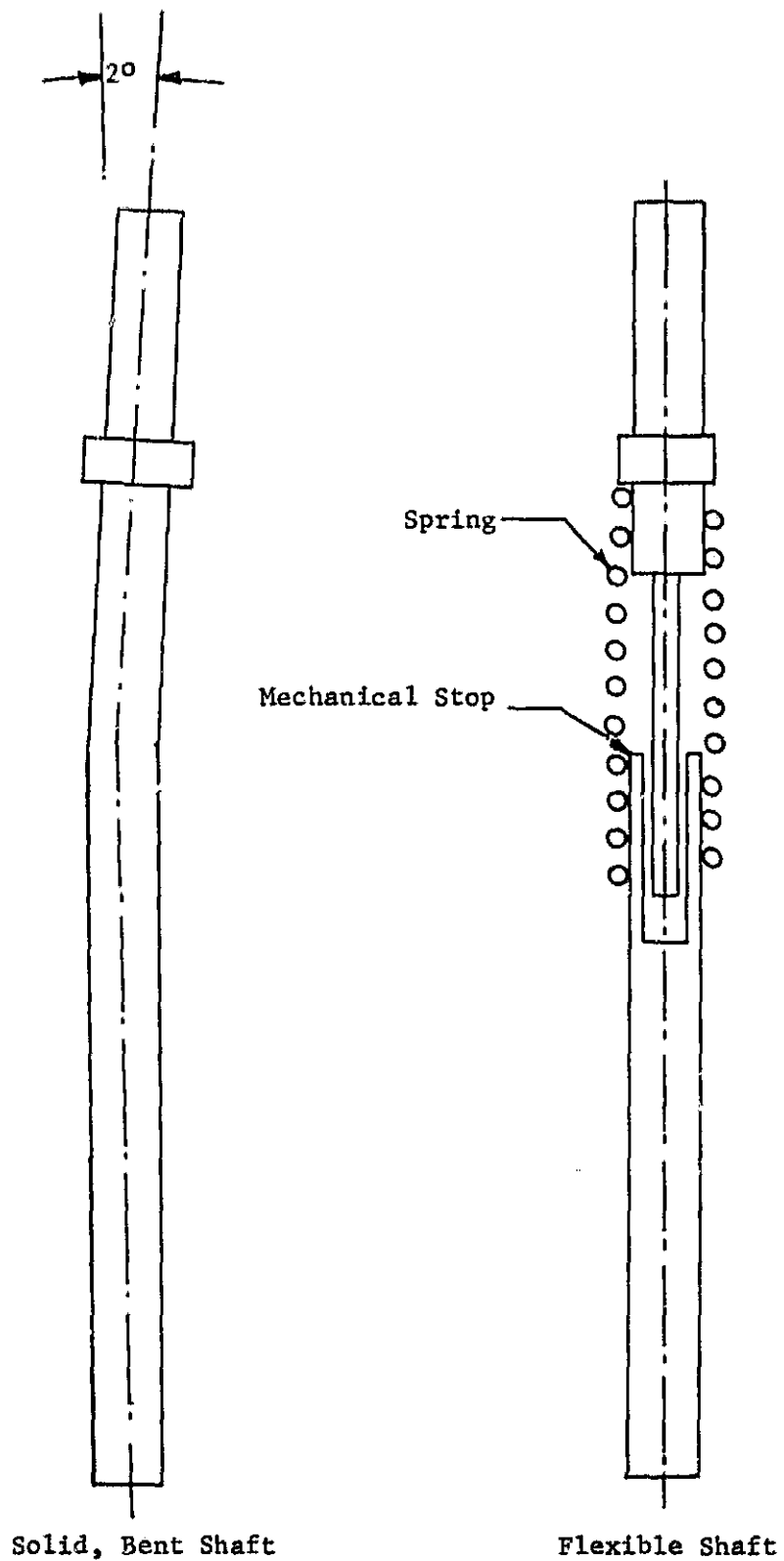
Figure 4:   Wobble Test Spin Shafts

geometric axis travel to $\pm2^O$. This method was used to ascertain whether perturbations and unsymmetrical liquid distributions would tend to increase the wobble effects. The helical spring used in the flexible coupling had an axial spring rate of 98.1 newtons/cm (56 lb$_f$/in.). A lateral force of approximately 0.556 newtons (0.125 lb$_f$) was required to hold the coupling against its mechanical stop.

Four types of tests were used to evaluate fluid behavior in a spinning toroidal tank. These were: ullage orientation, liquid settling, wobble, and spin rate change tests. A discussion of each of these types follows.

A. ULLAGE ORIENTATION

During the study described in Reference 1, a computer analysis indicated that the liquid-gas interface would be flat and the ullage uniformly distributed in the propellant tanks during all mission phases. This uniform distribution was attributed to the radial acceleration resulting from spin stabilization of the spacecraft. However, previous work performed at the NASA-LeRC Zero-G Facility (Ref. 5 and 6) indicated that, at liquid volumes of 50% or greater and under zero-g conditions without spin, the ullage in toroidal tanks tended toward an unsymmetrical orientation, forming one or more bubbles. Therefore, two aspects of the ullage behavior in toroidal tanks were to be investigated in the Martin Marietta Zero-G Facility. First, it was necessary to corroborate ullage-bubble breakup under zero-g conditions and then to evaluate the stabilizing effect of spin on the ullage orientation. The range of liquid volumes to be evaluated was specified at 5 to 96% of the total tank volume. Five volumes of 5, 25, 50, 75 and 96% were selected. A simulated propellant acquisition device of the type described in Reference 1 was included in the test tank.

The general procedure followed was to make two drop tests for each volume. The first test was conducted without spin. In the second test, the tank was spun at a given rate prior to and during the test. Both tests were conducted without axial acceleration. During each test, ullage behavior was recorded on high-speed color film.

To establish the required spin rate for the test tank and test fluid used, two similarity conditions are pertinent. The first is the tank Bond number and the second is the buoyancy force resulting from spacecraft spin. The Bond number is a dimensionless number defined as the ratio of hydrostatic to capillary forces acting at the liquid/vapor interface. It determines the shape of the liquid/vapor interface and provides an indication of the potential for ullage-bubble breakup. For example, at very low Bond numbers, the capillary forces predominate so that

the liquid/vapor interface is strongly curved with a high possibility of the ullage separating into two or more segments. At very high Bond numbers, the hydrostatic forces predominate so that the liquid/vapor interface is flat with essentially no possibility of forming or maintaining multiple bubbles. Mathematically, the Bond number is given by

$$B_o = \frac{\rho}{\sigma} L^2 A_t$$

where ρ = liquid density
σ = liquid surface tension
L = system characteristic dimension
A_t = total acceleration acting on the interface.

In the present test under zero-g conditions (no axial acceleration), the total acceleration is that resulting from spinning, i.e., the radial acceleration, given by

$$A_r = R\omega^2$$

where R = major toroidal radius
ω = spin rate.

If the characteristic dimension L is taken as the minor toroidal radius, r, the Bond number pertinent to the subject test is obtained from

$$B_o = \frac{\rho}{\sigma} r^2 R \omega^2,$$

Figure 5 shows the variation of Bond number with spin rate for each of the four specified propellants in the full-size tank defined in Reference 1. The pertinent propellant properties are summarized in Table 1. For the cruise spin rate of 5 rpm used in the Pioneer vehicle, the Bond numbers for the propellants range from about 40 for hydrazine to 300 for fluorine. For the higher spin rate of 10 rpm employed during ΔV engine firings, the corresponding Bond number variation is from 180 to 1200. According to Reference 7, for axisymmetric containers such as spheres or cylinders, the liquid/vapor interface is essentially flat at Bond numbers of approximately 50. Thus, the data of Figure 5 indicate that the hydrazine tank represents the worst case condition in regard to Bond number. To simulate these worst case conditions in the test tank, hydrazine tank Bond numbers were used to define test tank spin rates.
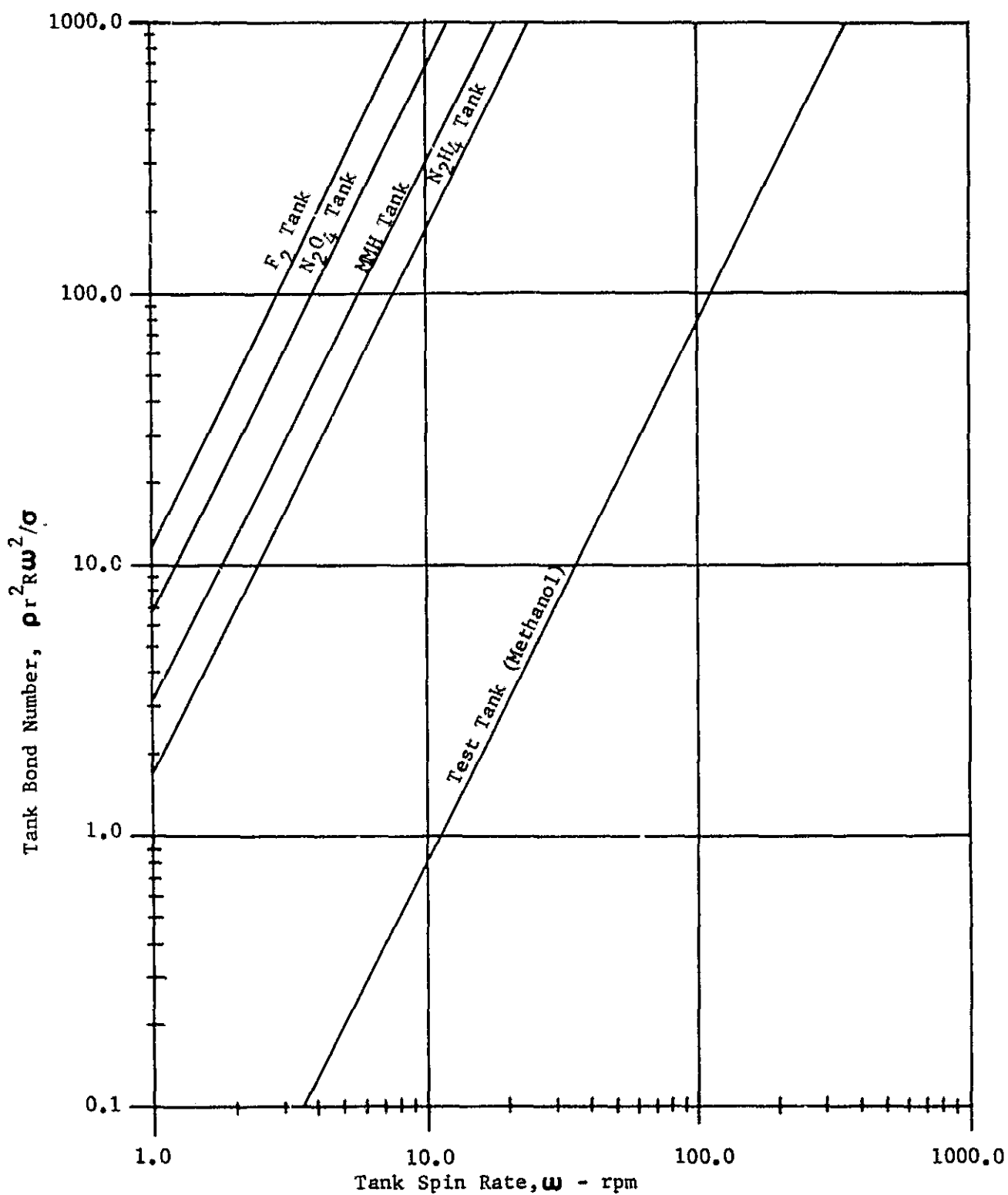
Figure 5: Variation of Tank Bond Number With Spin-Rate

Table 1: Fluid Property Summary

| Fluid	Density Kg/cm^3 (lb$_m$/ft^3)	Surface Tension Newtons/cm (lb$_f$/ft)
F$_2$	1.45 (90.5)	1.43×10^{-4} (0.97×10^{-3})
N$_2$O$_4$	1.45 (90.2)	2.69×10^{-4} (1.83×10^{-3})
MMH	0.88 (54.9)	3.44×10^{-4} (2.34×10^{-3})
N$_2$H$_4$	1.01 (62.8)	6.76×10^{-4} (4.6×10^{-3})
Methanol	0.79 (49.4)	2.28×10^{-4} (1.55×10^{-3})

The test fluid selected for the ullage orientation tests was methanol, primarily because its wetting characteristics are similar to the candidate propellants. Methanol properties are also presented in Table 1. Bond numbers for the test tank using methanol were calculated and are also shown in Figure 5 as a function of spin-rate. Simulating hydrazine tank Bond numbers at 5 and 10 rpm requires spinning the test tank at 75 and 150 rpm, respectively. While the lower spin rate is associated with a Bond number slightly less than 50, the higher spin-rate condition was selected for test. This higher spin rate represents the conditions just prior to starting the ΔV engine. If the ullage was unstable or unsymmetrical at this time, center-of-gravity shift might occur. Application of the ΔV engine thrust could create an attitude control problem. Therefore, the test spin-rate of 150 rpm was selected to simulate the higher Bond number condition which may have a more adverse affect on spacecraft operation. An unsymmetrical ullage at low spin-rates, while not desirable, was judged to be less critical because the long coast periods would allow reorientation of the ullage under the influence of spacecraft spin. This effect provides the basis for the second similarity condition which might be used to establish the test tank spin-rate. This condition is discussed in the following paragraphs.

The second similarity condition would require that the same buoyant force (i.e., radial acceleration) developed in the full-size tank be employed in the test tank. This radial acceleration, together with the test tank geometry, defines the spin rate necessary for similarity. However, tests performed under this condition would not be definitive. The radial acceleration during coast in the full-size tank at 5 rpm is 0.017g at the tank outer wall and decreases to one-half that value at the inner wall. The spin rate required to produce the same radial acceleration distribution in the test tank is 14 rpm. The Bond number in the test tank for this spin rate would be only 1.6 (see Figure 5). Thus, the ullage in the test tank could break-up into two or more bubbles as a result of splashing occurring during the change in axial acceleration from one-g to zero-g at the start of the drop test. The low buoyant force associated with the 14 rpm spin rate could then require time in excess of the 2.1-second drop time to orient the bubbles on the inner wall of the test tank. However, in the full-size tank under actual mission conditions, the Bond numbers are large (approximately 40 for the hydrazine tank) so that the possibility of ullage break-up is less. In addition, the time available between ΔV engine operations is measured in days so that any bubbles that might have been formed in the liquid from

the previous engine operation or other possible perturbations
would be moved by buoyancy toward the inner tank wall. Just
prior to firing the ΔV engine, the spacecraft spin r.e is in-
creased to 10 rpm with a corresponding four-fold increase in
buoyant force (radial acceleration). Any bubbles in the liquid
at that time should be moved rapidly to the inner tank wall.
Therefore, it is believed no problems due to ullage breakup will
occur in the full-size tank under normal operation of the pro-
posed spacecraft.

Results of the tests are presented in the following paragraphs.
Where possible, the discussion is supplemented by photographic
black-and-white enlargements of selected frames from the high-
speed color films.

In general, the test results were in agreement with the results
of References 5 and 6. For liquid volumes of 50% or greater
under conditions of zero-g, the ullage tended toward an unsym-
metrical distribution and, in some cases, broke up into several
bubbles. Applying a spin rate of 150 rpm to all volume condi-
tions produced a stable, symmetrical ullage under zero axial-g
conditions. Figure 6 illustrates the ullage orientation for a
96% liquid volume for a zero rpm spin rate under both one-g and
zero axial-g acceleration conditions. In Figure 6(a), the
system is subjected to a normal one-g environment prior to the
drop test and the ullage is distributed symmetrically in the top
of the tank. Figure 6(b) is a picture taken near the end of the
2.1-second, zero-g drop test for the 96% liquid volume. The
ullage volume has divided into seven distinct bubbles which are
non-symmetrically distributed in the tank. Figure 7 presents
similar data for 96% liquid volume subjected to a spin rate of
150 rpm. Under a one-g acceleration, the liquid is displaced to
the outer wall with the ullage located nearer to and symmetrical
about the spin axis as indicated in Figure 7(a). A theoretical
propellant distribution for these conditions is shown in Figure 8,
assuming the liquid-gas interface is flat. Comparison of the
photograph of Figure 7(a) with the drawing of Figure 8 shows
good agreement in regard to liquid distribution and orientation.
For the condition of zero axial acceleration with spin, the
liquid-gas interface should be oriented vertically or parallel
to the spin axis, since only radial acceleration is present.
The ullage should also be uniformly distributed. Figure 7(b),
taken from the film strip near the end of the drop test, shows
that these conditions do exist. In the tank top view in Figure
7(b), the liquid-gas interface appears as a circle near the
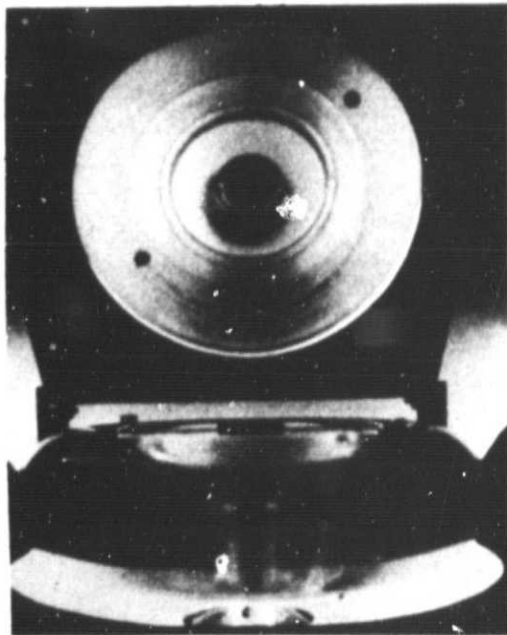toroidal tank inner wall.
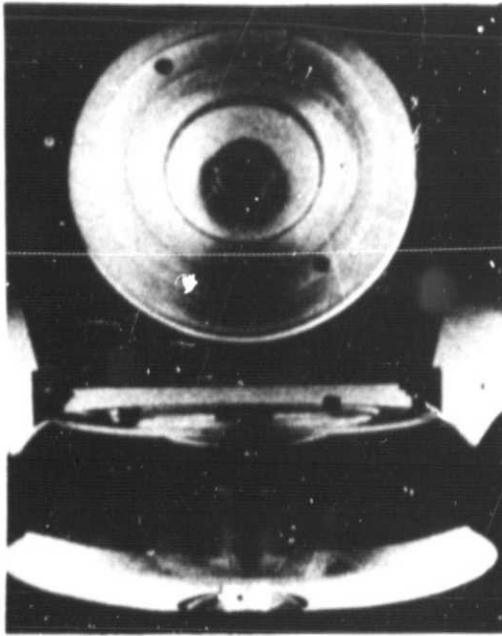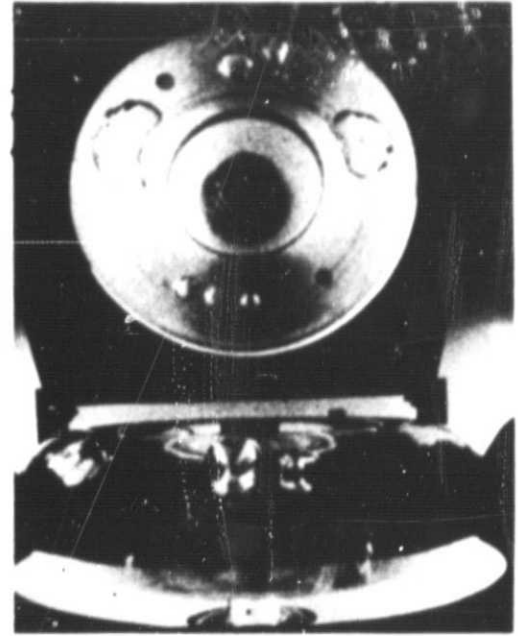
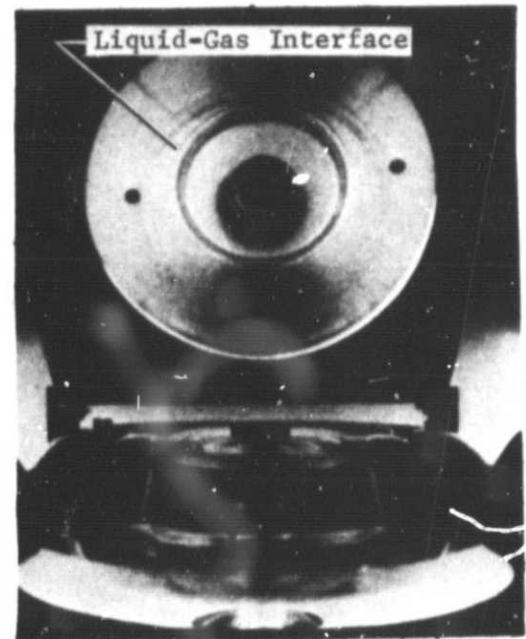(a)   Axial Acceleration = One-g   (b)   Axial Acceleration = Zero-g

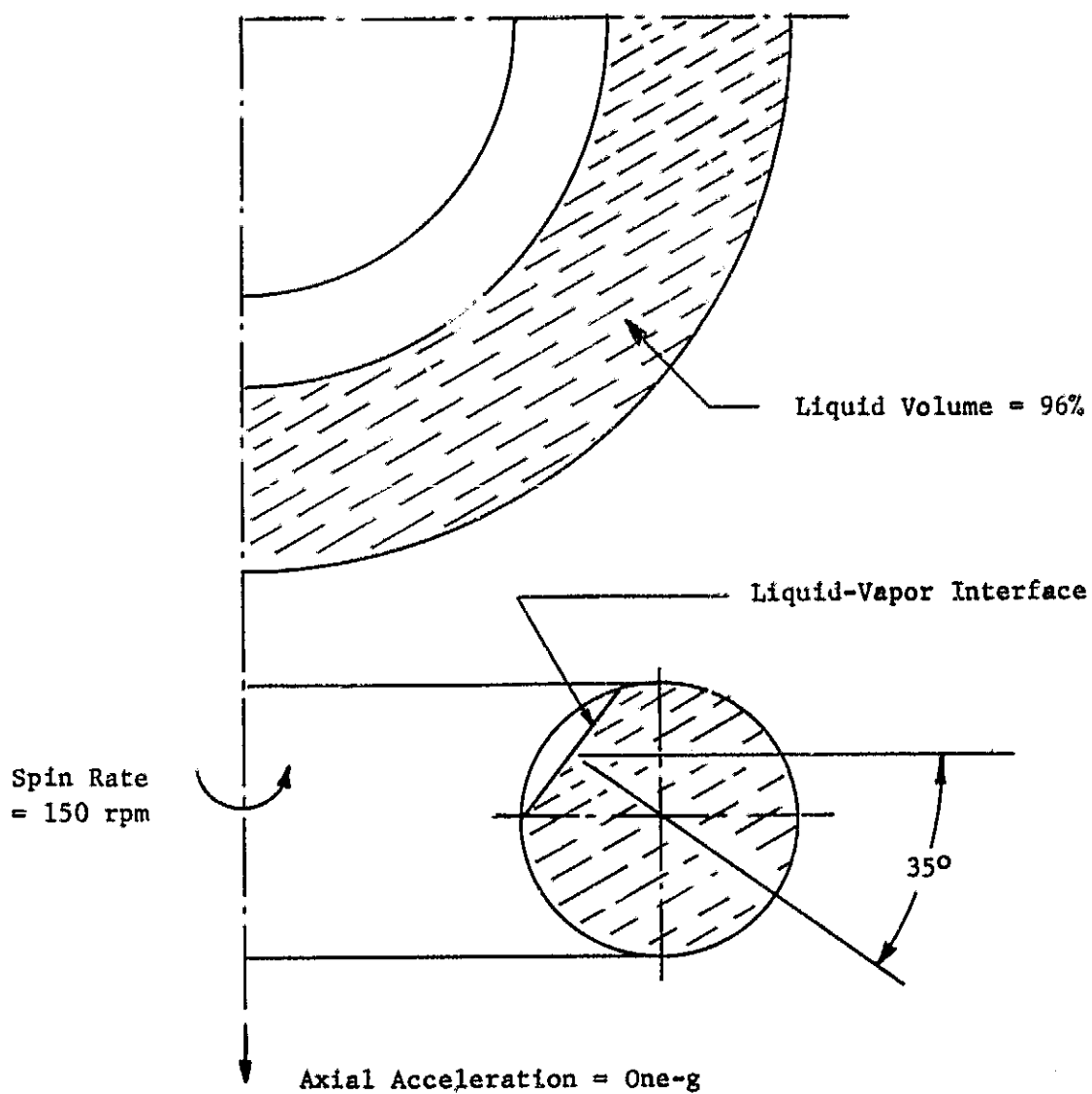Figure 6: Ullage Orientation for 96% Liquid Volume and Zero rpm Spin-Rate

(a)   Axial Acceleration = One-g   (b)   Axial Acceleration = Zero-g

Figure 7: Ullage Orientation for 96% Liquid Volume and 150 rpm Spin Rate

Liquid Volume = 96%

Liquid-Vapor Interface

Spin Rate
= 150 rpm

35°

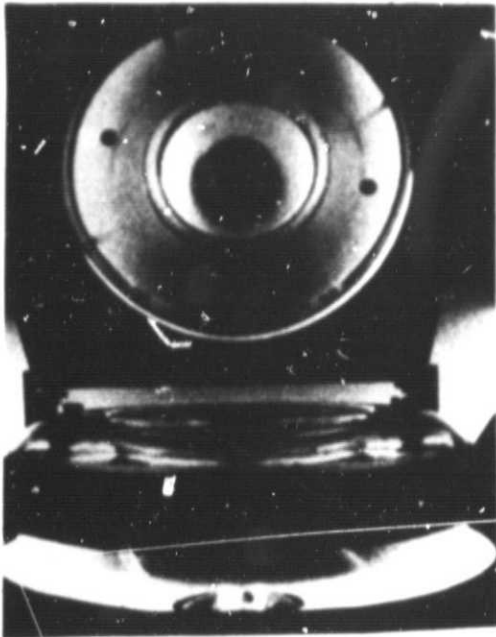Axial Acceleration = One-g

NOTE: Drawing is Full-Size

Figure 8: Theoretical Propellant Distribution in the Test Tank

Test results for the cases of 75% liquid volumes with no spin and with spin are shown in Figures 9 and 10, respectively. Comparison between Figure 9(b) and Figure 10(b) shows the stabilizing effect of spin on the ullage orientation in a zero axial-g environment. In Figure 9(b) the ullage volume is unsymmetrical, forming a bubble roughly in the shape of a toroidal segment. With the application of spin, the ullage as shown in Figure 10(b) is symmetrically distributed about the spin axis on the tank inner wall.

Figures 11 and 12 present results of testing with a liquid volume of 50%. The photograph of Figure 11(b), taken near the end of the drop test, indicates that unsymmetrical distribution was beginning to develop. Had test time been longer, one or more bubbles in the shape of toroidal segments would probably have formed. As for previous volumes, the application of spin produced a symmetrical distribution of the ullage volume on the inner toroidal tank surface, as indicated in Figure 12.

Testing with 25 and 5% liquid volumes produced results somewhat different in that the propellant distribution and, therefore, the ullage was symmetrical under conditions of zero axial acceleration and zero spin rate. These results are in agreement with those of References 5 and 6. Figure 13 shows the propellant distribution for 25% liquid volumes during zero-g drop tests without and with a spin rate. In both cases, most of the liquid is distributed on the outer tank wall. In Figure 13(a), a small amount of liquid is distributed at the top and bottom of the tank as indicated by the slight shading. However, with the 150 rpm spin rate, all of the liquid is distributed on the outer tank surface.

Figure 14 shows the liquid distribution for the 5%-volume tests. For a zero spin rate, Figure 14(a) shows that nearly all of the liquid is retained around the edges of the propellant acquisition device. This result indicates that, although the propellant acquisition device was designed to function under the influence of a radial acceleration, it will also retain some propellant under the resulting zero-g condition if it were necessary to completely despin the spacecraft. When the 150 rpm spin rate was applied to the tank, the liquid was distributed on the outer tank surface as shown in Figure 14(b). The liquid mass was still in contact with the communication channels of the propellant acquisition device.
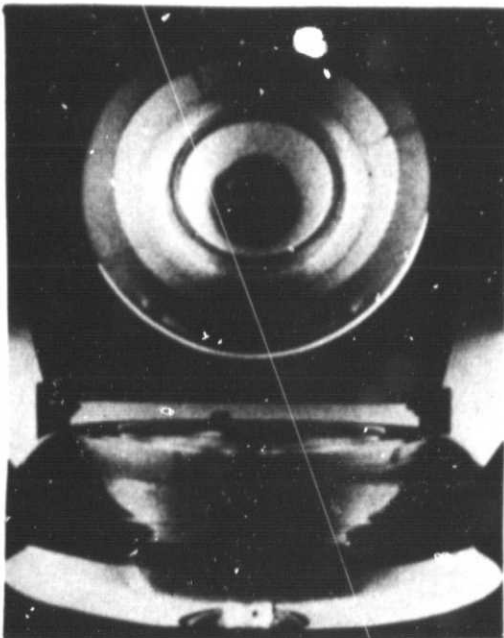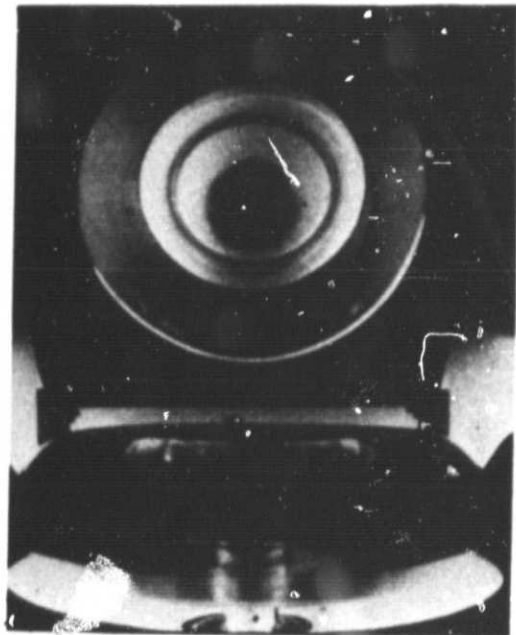
(a) Axial Acceleration = One-g
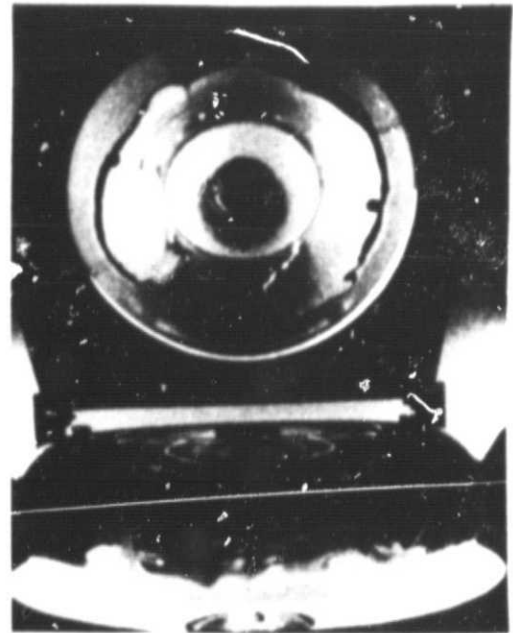
(b) Axial Acceleration = Zero-g

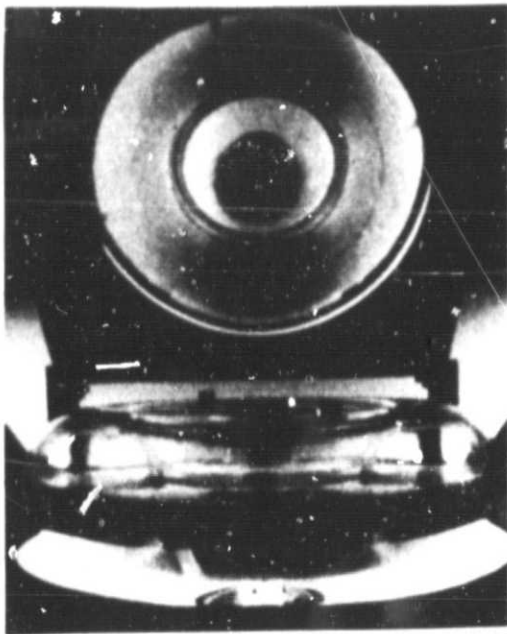Figure 9: Ullage Orientation for 75% Liquid Volume and Zero rpm Spin-Rate

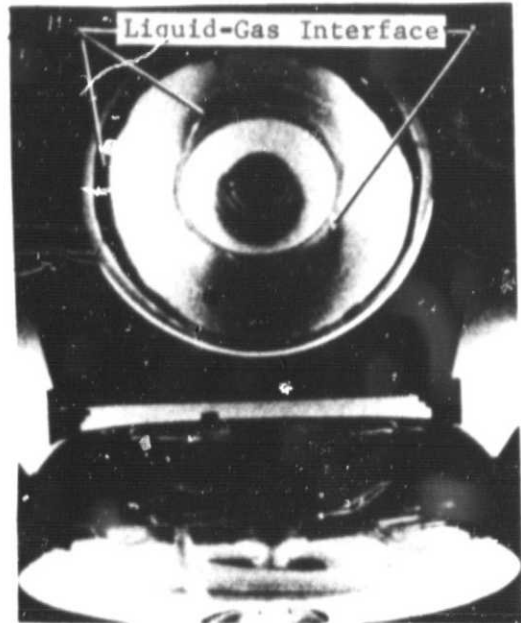
(a) Axial Acceleration = One-g

(b) Axial Acceleration = Zero-g

Figure 10: Ullage Orientation for 75% Liquid Volume and 150 rpm Spin-Rate
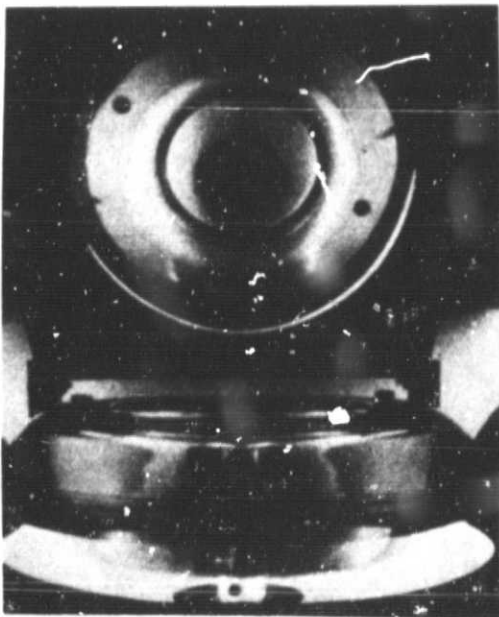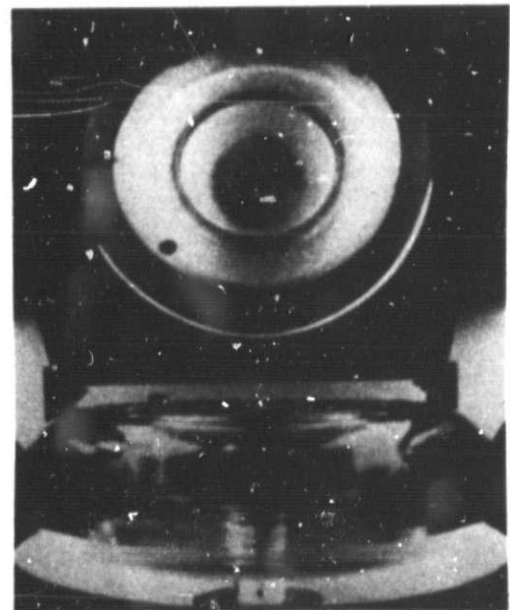
19

(a) Axial Acceleration = One-g

(b) Axial Acceleration = Zero-g

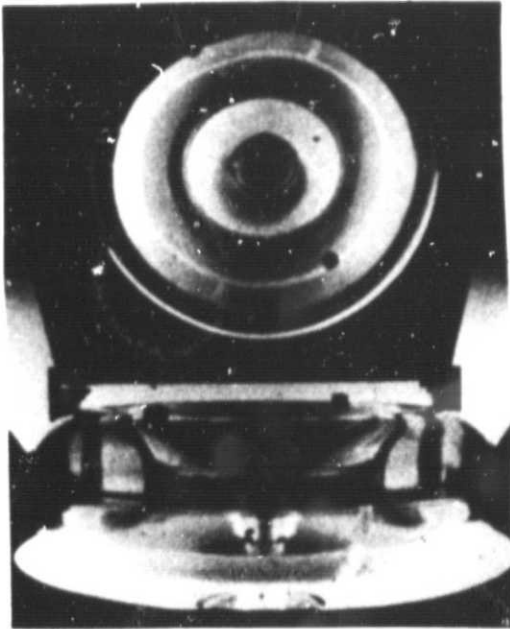Figure 11: Ullage Orientation for 50% Liquid Volume and Zero rpm Spin-Rate
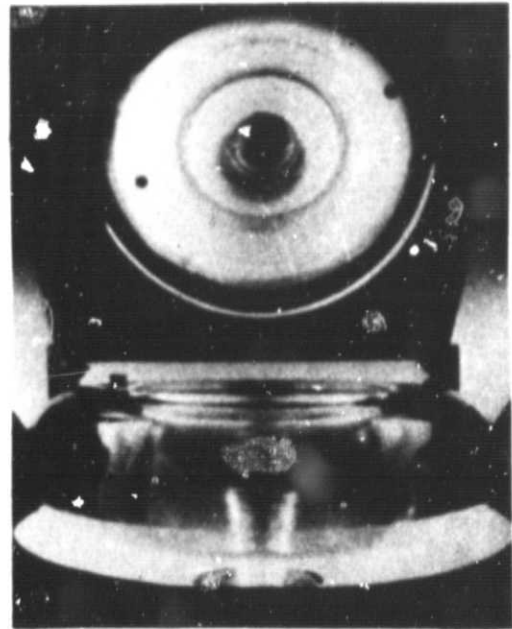

(a) Axial Acceleration = One-g

(b) Axial Acceleration = Zero-g

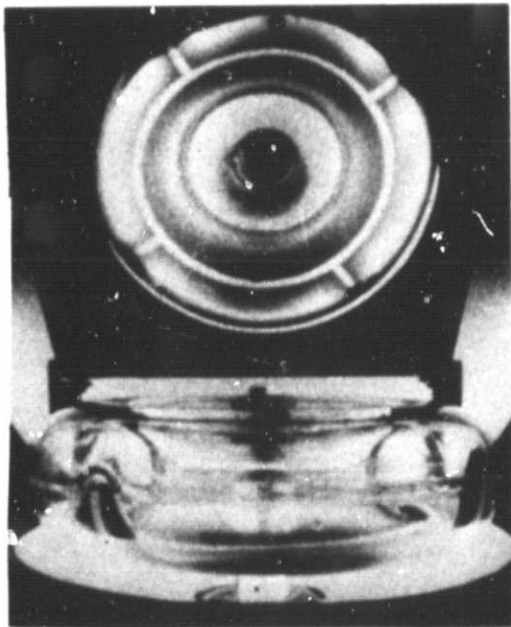Figure 12: Ullage Orientation for 50% Liquid Volume and 150 rpm Spin-Rate
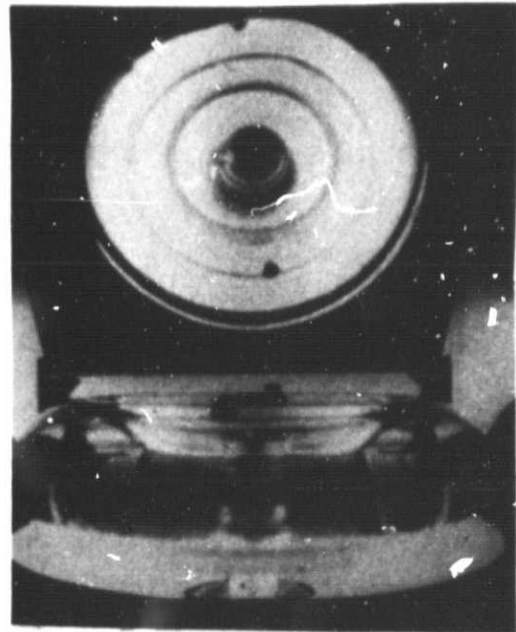
(a) Zero rpm Spin-Rate

(b) 150 rpm Spin-Rate

Figure 13:   Ullage Orientation for 25% Liquid Volume and Zero Axial
Acceleration

(a) Zero rpm Spin-Rate

(b) 150 rpm Spin-Rate

Figure 14:   Ullage Orientation for 5% Liquid Volume and Zero Axial
Acceleration

B.   LIQUID SETTLING

It was shown during the ullage orientation analysis, described in
Reference 1, that the propellant mass in the toroidal tank prior
to engine firing (zero axial acceleration) is distributed on the
outer surface of the tank wall. This particular distribution is
a result of the prevailing radial acceleration due to spacecraft
spin. When the engine is started, the propellant mass moves in
response to the axial acceleration component toward the bottom of
the tank and up the inner tank wall. A simplified slosh analysis
conducted during the previous study showed that significant damp-
ing of the propellant motion was provided by the recommended pro-
pellant acquisition device. To verify these analytical results,
the liquid settling process was simulated in the drop tower.
Test conditions employed were:

1)   Liquid volumes of 5, 25, and 50%;

2)   Axial acceleration of 0.034g;

3)   Spin rates of 15, 20, 25, and 50 rpm; and,

4)   Methanol as the test fluid.

The liquid volume range tested was selected on the assumption that
sloshing forces arising from liquid settling in the toroidal tank
would increase to a maximum at liquid volumes of 50%, as is the
case in spherical tanks (Ref. 4). The axial acceleration specified
above is the maximum value that could be readily applied in the
drop tower facility with available equipment. This acceleration
was provided by clustering three 22.24-newton (5-lb$_f$) NEG'ATOR
springs in parallel. The resulting force of 66.72-newtons (15-
lb$_f$), when divided by the total test cell mass of 199 kilograms
(439 lb$_m$), produced an average acceleration of 0.034g.

In order to maintain similarity between the scale model and full-
size system operation, the ratio of axial to radial accelerations
of the full-size tank was used to establish test model spin rates.
An estimate of this ratio was made from mission data given in
Reference 1. The result is plotted versus percent liquid volume
in Figure 15. It was also desired to extend the coverage of the
test program to provide parametric data. A second acceleration-
ratio variation based on increased propellant mass, spacecraft
spin rate, and engine thrust was also estimated and is plotted
as the parametric curve in Figure 15. The spacecraft data used
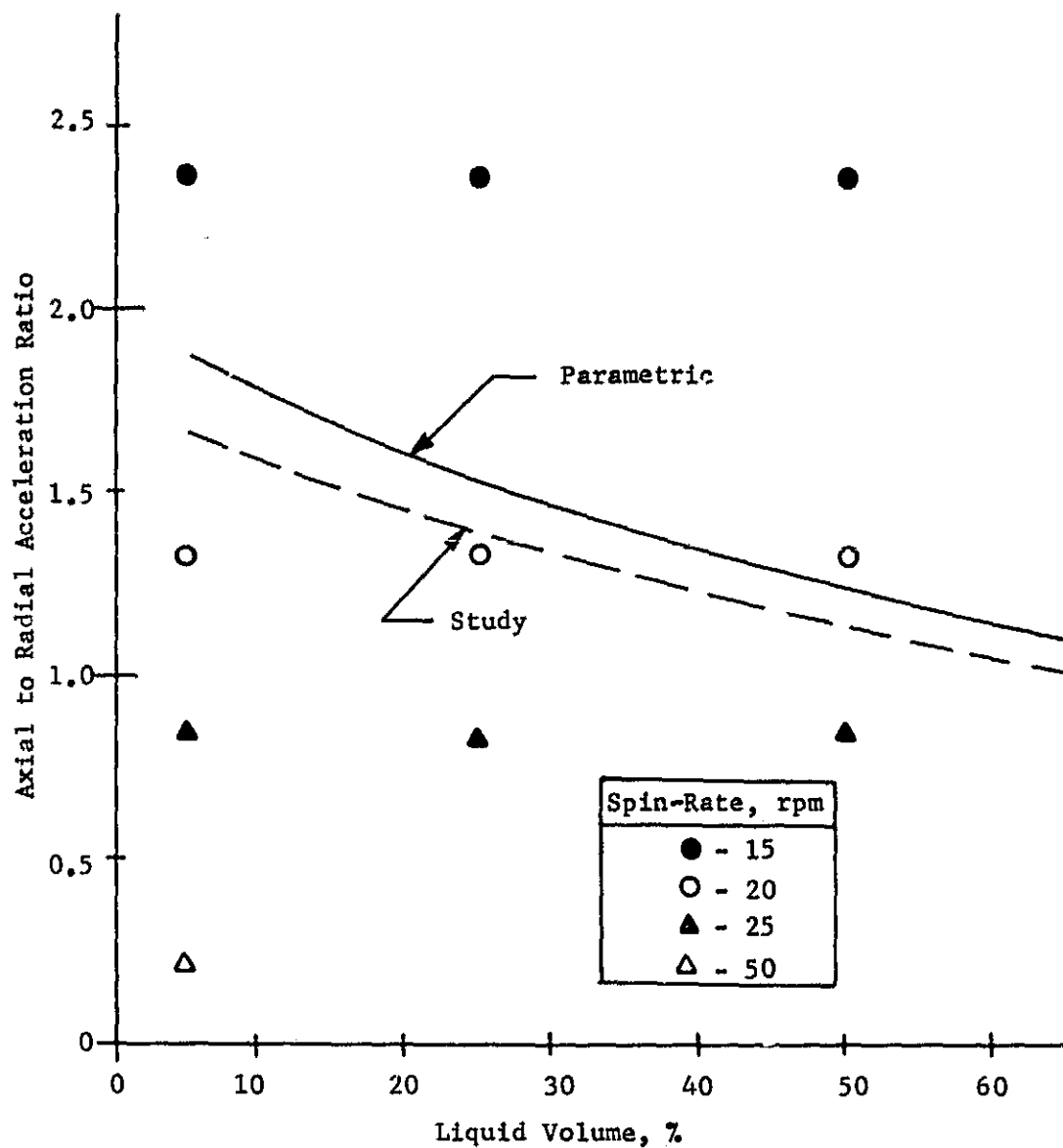to calculate the two acceleration-ratio curves is presented in
Table 2.

Figure 15: Axial to Radial Acceleration Ratio for
            Liquid Settling and Slosh Analysis

Table 2: Spacecraft Data Used to Calculate Acceleration Ratios

|	Study	Parametric
Propellant Mass, Kg (lb$_m$)	472 (1040	590 (1300)
Spacecraft Mass, Kg (lb$_m$)	939 (2069)	1043 (2300)
Maximum Spin Rate, RPM	10	20
Maximum Axial Acceleration, g	0.091	0.4
Tank Geometry		
Minor Radius, m (ft)	0.154 (0.505)	0.154 (0.505)
Major Radius, m (ft)	0.458 (1.505)	0.458 (1.505)

The spin rates for the test program were selected to bracket the
two acceleration lines. Tests were performed with 5, 25, and 50%
liquid volumes at spin rates of 15, 20, and 25 rpm, as indicated
in Figure 15. A test was also run for the 5% liquid volume case
at a 50-rpm spin rate. For each drop test, the test tank was
mounted in the test cell in an inverted position so that the
bottom half of the tank (the half with the propellant acquisition
device) was uppermost. The tank was positioned in this manner
since the NEG'ATOR spring imparts a downward acceleration on the
test cell, as indicated in Figure 2. This downward pull represents
the axial engine thrust and tends to move the liquid upward during
the drop test. In subsequent discussions, the portion of the tank
with the simulated propellant acquisition device will be referred
to as the bottom half regardless of the orientation in the drop
tests. The NEG'ATOR spring force was applied to the test cell at
the start of the test and continued until the test cell bottomed
in the arrestor inside the drag shield near the end of the drop
period. Prior to initiating the drop test, the desired spin rate
was applied to the toroidal tank. This spin rate was also
applied continuously during the test. An additional test was
conducted without a simulated propellant acquisition device to
allow a comparison of the settling and slosh damping in the
toroidal tank with and without a propellant acquisition device.
This test was conducted at a 25% liquid volume and a spin rate
of 20 rpm.

The results indicate that, in general, no major slosh problems
would be associated with propellant settling in the toroidal tank
system of a spin-stabilized vehicle. Most of the fluid oscilla-
tions in the model tanks with the propellant acquisition device
appeared to be reasonably damped by the end of the test time.
To illustrate these results, a series of sequential photographs
was made from the high-speed film strips of four drop tests.
These four tests were selected as being representative of the
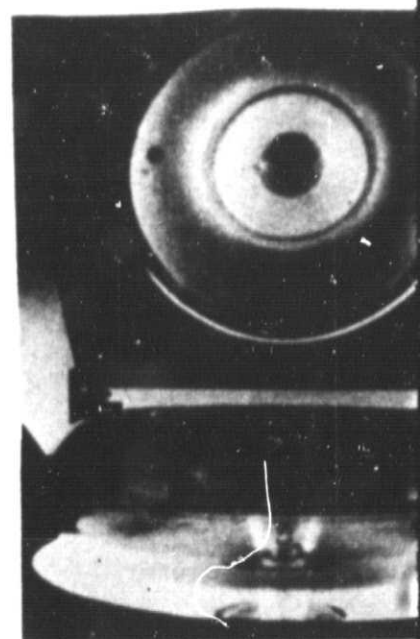entire liquid settling tests.

Figure 16 presents the sequential photographs for the first test
in which the tank does not contain a propellant acquisition de-
vice. Figure 16(a) illustrates the orientation of the liquid
just before the drop test was initiated. At this time, the axial
acceleration is effectively negative with a magnitude of normal
gravity and the liquid is located in the top of the inverted tank.
The spin rate of 20 rpm produces a radial acceleration of only
0.026g (at the major radius) so that displacement of the liquid
toward the outer wall is not discernible (i.e., the liquid-gas
interface is essentially horizontal). Figure 16(b) shows the
orientation of the liquid at 0.5 second. By this time, the liquid
has moved under the combined positive axial and radial acceler-
ations from the top of the tank, along the outer wall to the
bottom of the tank, and toward the inner wall, as is indicated
by the dark areas in the top and front views. After 1.0-second,
the liquid has reversed its direction and is moving back toward
the outer tank wall as indicated by the darkening front view in
Figure 16(c). By 1.5 seconds, as indicated in Figure 16(d),
most of the liquid has been displaced to the outer wall in the
bottom half of the tank under the combined effect of axial and
radial acceleration. The lack of propellant on the inner surface
is evident by the very light areas in the center of the top view
and the lower part of the front view. At 2.0 seconds, just be-
fore the end of the test, the liquid has again reversed its
direction of motion and is moving toward the inner walls. This
is indicated by the darkening areas in the bottom of the tank in
Figure 16(e).

The photographic sequence indicates that an oscillatory or slosh-
ing motion of the liquid is present. Since the drag force along
the walls, the liquid internal friction, and the capsule total
acceleration are all small, this motion would continue for some
time. The 2.1-second drop test time is not sufficient for these
forces to damp out this motion. A very rough estimate of the
frequency of the oscillation was made by observing the liquid-
gas interface movement along the tank surface in the top view.
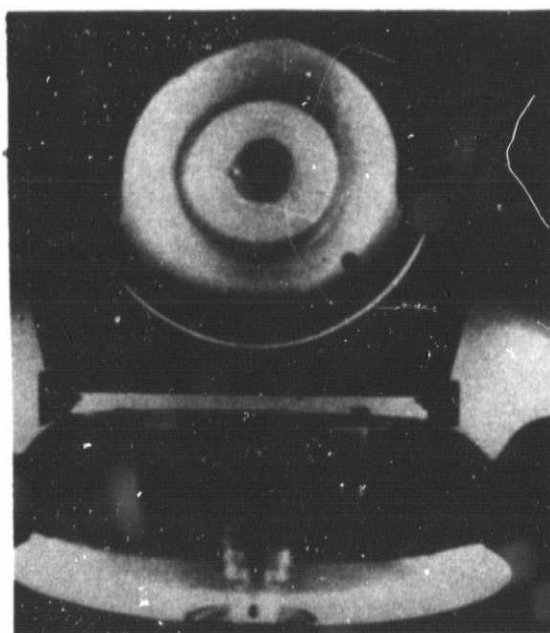This interface appeared as a distinct line in the top view moving
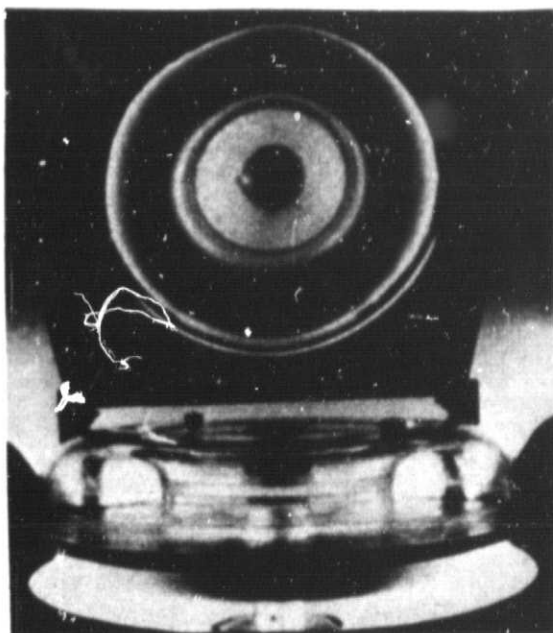
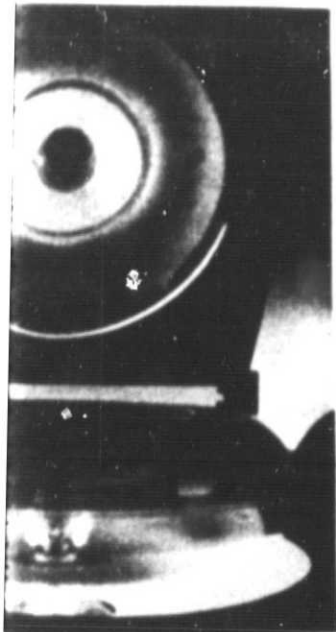(a) Time = Zero Sec.
     Axial Acceleration = 1.0g

(b) Time = 0.5 Sec.
     Axial Acceleratio
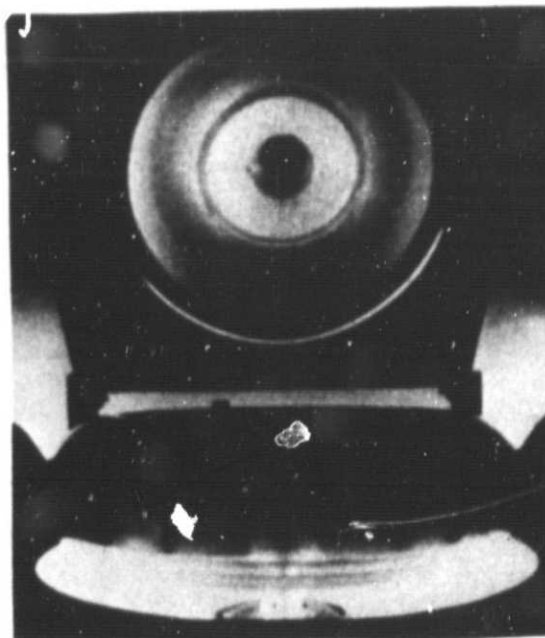

(d) Time = 1.5 Sec.
     Axial Acceleration = 0.034g
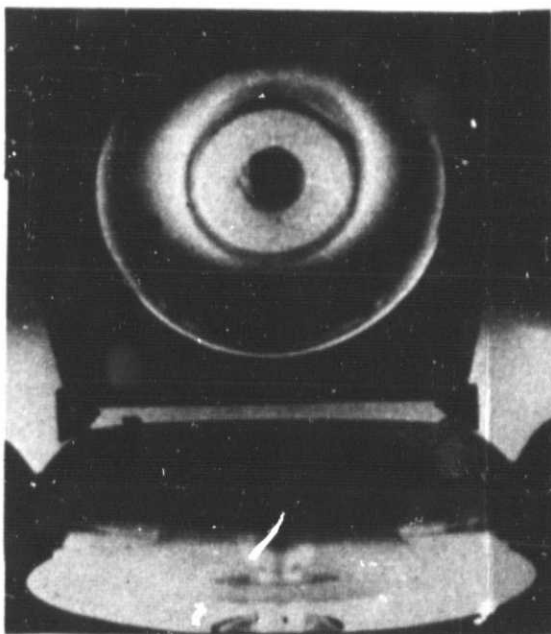
Figure 16:   Liquid Settling Test Without a Propellant A

0.5 Sec.
Acceleration = 0.034g

(c) Time = 1.0 Sec.
Axial Acceleration = 0.034g
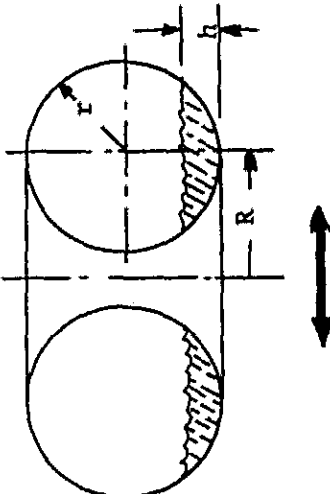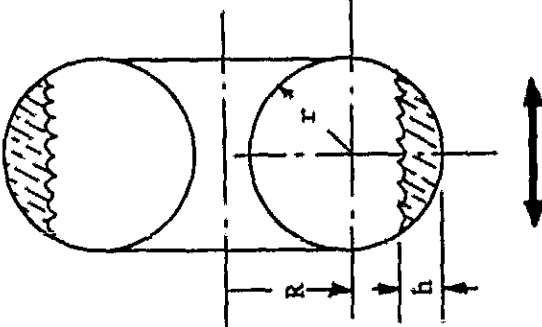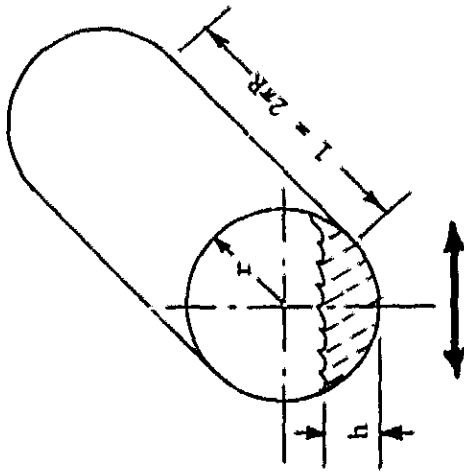

(e) Time = 2.0 Sec.
Axial Acceleration = 0.034g

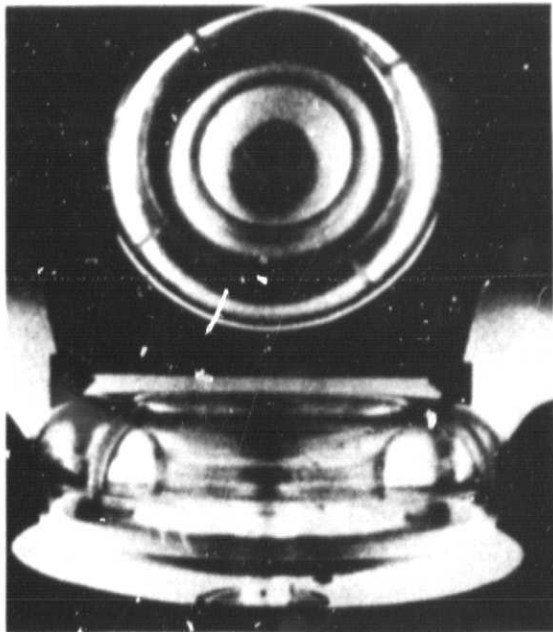Propellant Acquisition Device (Liquid Volume = 25%, Spin-Rate = 20 rpm)

from the outer tank wall to the inner wall and returning to the outer wall. The estimate of the frequency was obtained by dividing the camera speed (200 frames/sec) by the total number of frames exposed during the travel of the interface from the outer wall to the inner wall and back to the outer wall. A natural frequency of 0.77 cycles/sec was obtained for liquid sloshing in the spinning toroidal tank by averaging several readings.

A review of previous slosh analysis and testing in toroidal tanks was made for comparison. All previous work has been performed under non-spinning conditions. Three possible methods for calculating natural frequencies were identified from the review. The first two methods were obtained from Reference 8 for toroidal tanks in two different orientations. The third method employed data for a horizontal circular canal from Reference 4, as an approximation for the torus. Table 3 describes the tank orientations and data used in calculating the natural frequencies. The liquid volume assumed in each case was 25%. In the second method with the torus mounted vertically, an assumption regarding propellant distribution had to be made. The height of liquid, h, used to calculate the natural frequency was assumed to be equal to that value that would exist when the liquid is distributed uniformly in a spinning tank. In the testing reported in Reference 8, the value of h was the actual height of the liquid volume lying in the bottom of the tank. The calculated natural frequencies for the latter two methods in Table 3 show remarkable agreement with the estimate from the film strip. It may be that these methods will provide reasonable estimates of natural frequencies for sloshing analysis in spinning toroidal tanks. However, more testing is obviously required to justify use of these methods.

Additional liquid settling tests were performed with a simulated propellant acquisition device installed in the tank to evaluate the ability of the device to retard or damp out slosh motions. In Figure 17, the results of the second drop test (5% liquid, 20 rpm) are shown at various times during the drop. Figure 17(a) illustrates the liquid orientation at the beginning of the test. After approximately 0.76 second, the liquid has moved from the tank top and impacted on the retaining ring of the propellant acquisition device at the bottom of the inverted tank, as indicated in Figure 17(b). No further liquid movement past the retaining ring toward the inner tank wall is noted in subsequent frames. In other words, this part of the propellant acquisition device stops the advancement of the liquid toward the bottom of the tank allowing the liquid to accumulate in the bottom half of the tank outside of the retaining ring. Figures 17(c) and 17(d) illustrate this condition. The size of the retaining ring is sufficient to retain the small quantity of liquid in this position.

Table 3: Models Used to Calculate Natural Frequencies

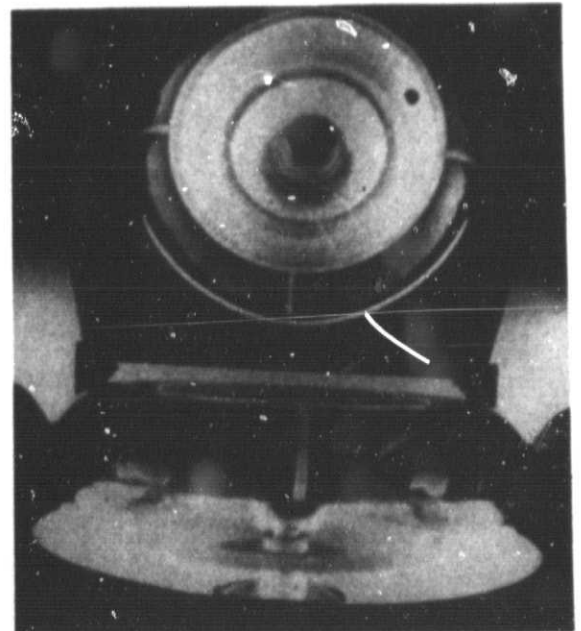| Source of Information	TN D-531 (Ref. 8)	TN D-531 (Ref. 8)	NASA SP 106 (Ref. 4)
Assumed Data	$r = 0.75$ in. $R = 2.25$ in. $V = 25\%$ $h = 0.44$ in. $a = 0.043g$	$r = 0.75$ in. $R = 2.25$ in. $V = 25\%$ $h = 0.385$ in. $a = 0.043g$	$r = 0.75$ in. $R = 2.25$ in. $l = 2\pi R = 14.14$ in. $V = 25\%$ $h = 0.44$ in. $a = 0.043g$
Calculated Natural Frequencies	0.15 cps	0.79 cps	0.81 cps

28

(a) Time = Zero Sec.
Axial Acceleration = 1.0g
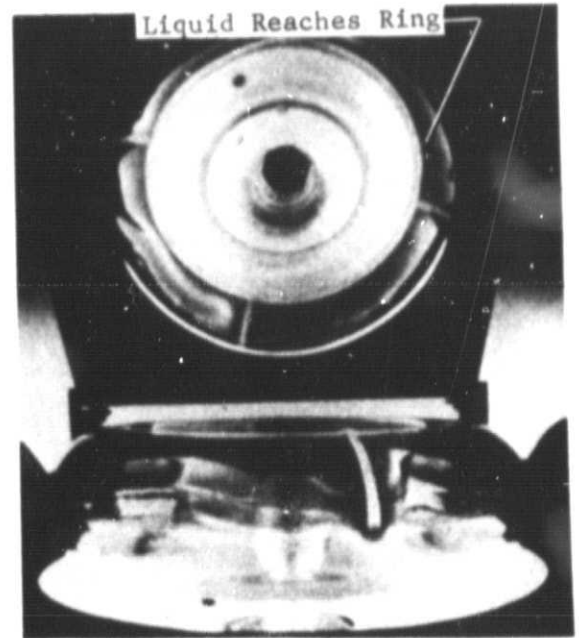
(b) Time = 0.76 Sec.
Axial Acceleration = 0.034g
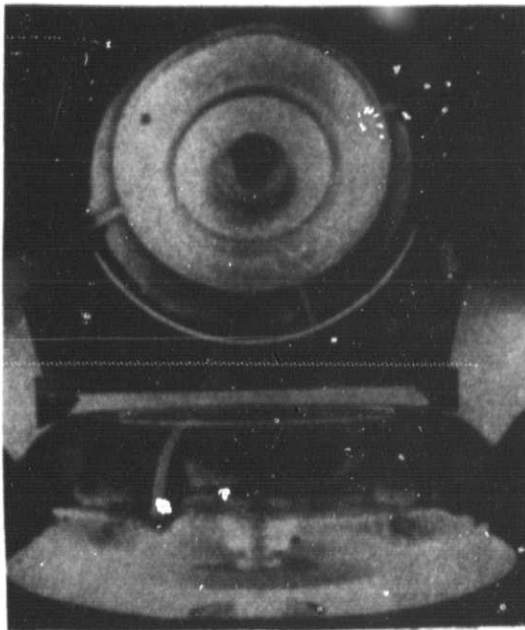
(c) Time = 1.0 Sec.
Axial Acceleration = 0.034g

(d) Time = 1.5 Sec.
Axial Acceleration = 0.034g

Figure 17:   Liquid Settling Test With a Propellant Acquisition
Device (Liquid Volume = 5%, Spin-Rate = 20 rpm)

For the third settling test, a liquid volume of 25% was used.
The corresponding photographic sequence of the liquid motion is
shown in Figure 18. Figure 18(a) shows the liquid orientation at
the start of the test. Approximately 0.36 second after initiating
the drop test, the liquid-gas interface has moved up the outer
wall and contacted the retaining ring of the propellant acqui-
sition device as shown in Figure 18(b). After 0.5 second, the
liquid continued to accumulate against the retaining ring as
indicated by the darkening areas in the top and front view of
Figure 18(c). At approximately 0.75 second, sufficient liquid
mass has accumulated behind the retaining ring so that the liquid
began to overflow the ring toward the spin axis of the tank. At
1.0 second, the darkened areas inside the ring in Figure 18(d)
illustrate that a small quantity of liquid has accumulated inside
the ring. After 1.5 seconds, the liquid orientation appears to
be stabilized and all significant liquid movement damped out.
The liquid orientation and distribution at 1.5 seconds is shown
in Figure 18(e).

The results of the drop test with 50% liquid volume are shown
in Figure 19. Because of the larger mass of liquid, a shorter
time interval, 0.27 second, was required for the liquid-gas
interface to reach the retaining ring shown in Figure 19(b).
After 0.5 second of test time had elapsed, a significant amount
of liquid had spilled over the retaining ring as shown by the
dark areas in the top view of Figure 19(c). At 1.0 second, the
liquid appears to be uniformly distributed in the bottom half of
the tank (Figure 19(d)). However, fluid motion is still observed
on the liquid-gas interface in the lower half of the front view
of the tank. After 1.5 seconds, the liquid has moved to an area
between the retaining ring and the tank outer diameter in the
bottom half of the tank (Figure 19(e)). Near the end of the test
at 2.0 seconds, some of the liquid had moved back toward the spin
axis as indicated by the darkened central portion of the tank top
view in Figure 19(f). It appears that some fluid motion still
was present at the end of the drop test with a 50% liquid volume.

An evaluation of the films from those drop tests employing spin
rates other than 20 rpm was also made. Since the results were
essentially the same as for the 20 rpm tests, photographic data
for these tests are not included in this report. One exception
that should be discussed is the test of a 5% liquid volume at a
spin rate of 50 rpm. This particular test was the only one per-
formed at the higher spin rate. From the start of the test, the
liquid-gas interface moved rapidly to impact the retaining ring
in 0.34 seconds. After impacting on the retaining ring, the
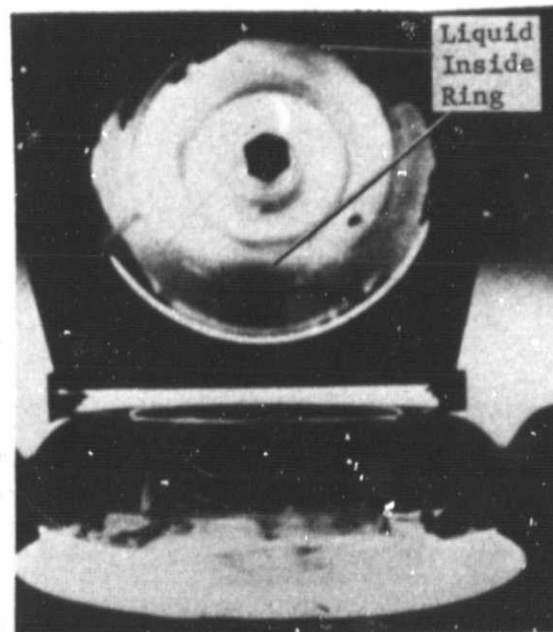fluid reversed its direction of motion and moved to the outer
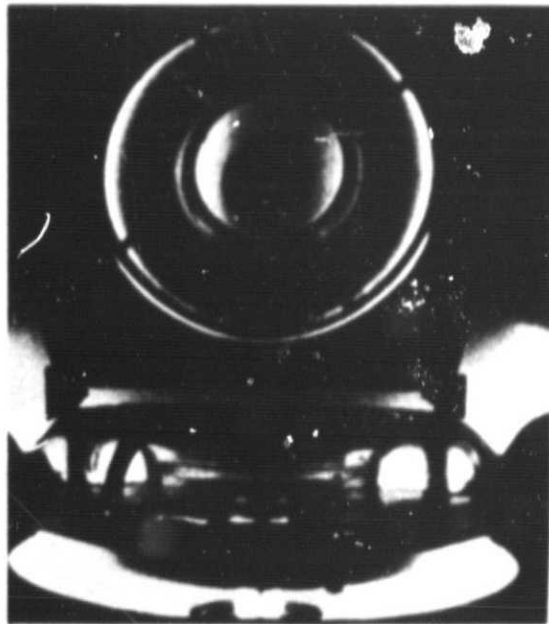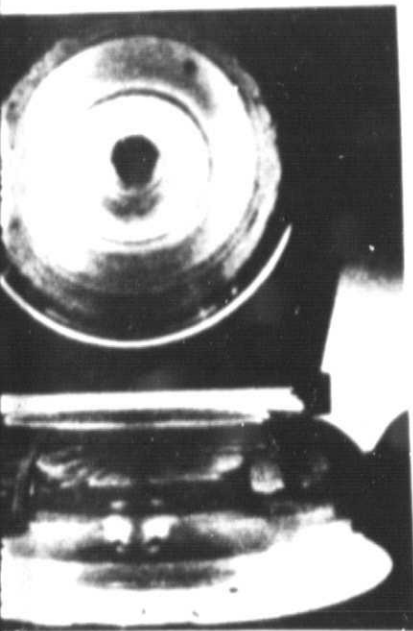
(a) Time = Zero Sec.
     Axial Acceleration = 1.0g

(b) Time = 0.36 Sec.
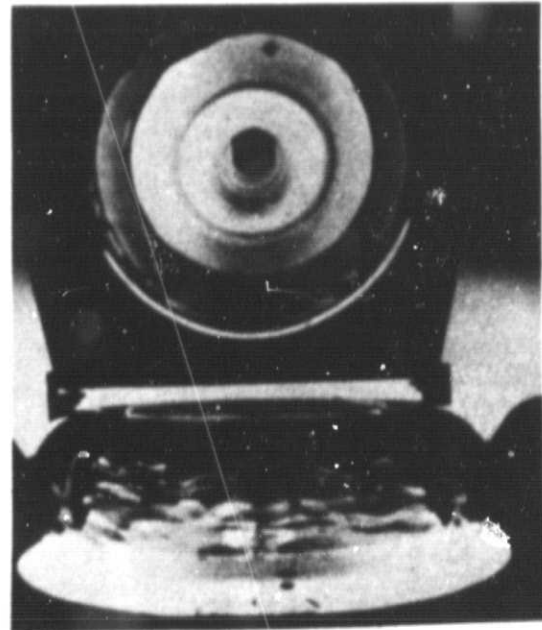   Axial Acceleration

Liquid
Inside
Ring

(d) Time = 1.0 Sec.
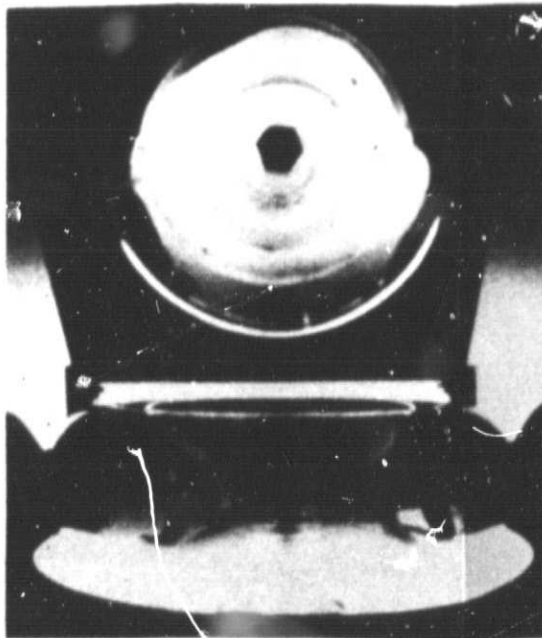   Axial Acceleration = 0.034g

Figure 18: Liquid Settling Test
            Device (Liquid Volum

ime = 0.36 Sec.
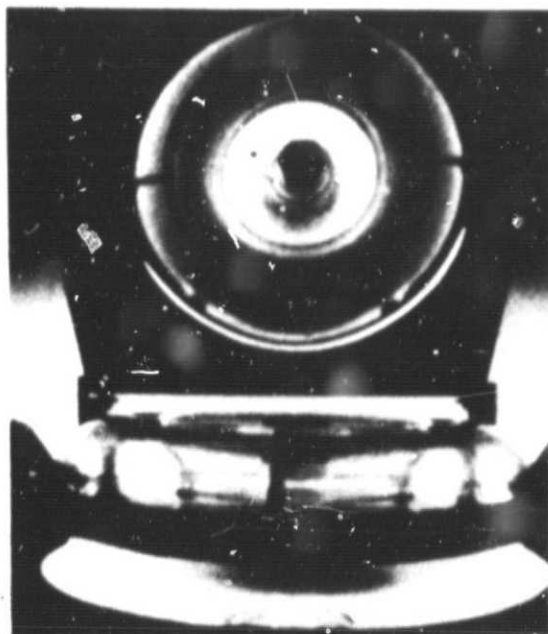xial Acceleration = 0.034g

(c)   Time = 0.5 Sec.
      Axial Acceleration = 0.034g

(e)   Time = 1.5 Sec.
      Axial Acceleration = 0.034g

uid Settling Test with a Propellant Acquisition
ice (Liquid Volume = 25%, Spin-Rate = 20 rpm)

31

(a) Time = Zero Sec.
Axial Acceleration = 1.0g

(b) Time = 0.27 Sec.
Axial Acceleration

(d) Time = 1.0 Sec.
Axial Acceleration = 0.034g

(e) Time = 1.5 Sec.
Axial Acceleration

Figure 19: Liquid Settling Test wi
(Liquid Volume = 50%, S

Time = 0.27 Sec.
Axial Acceleration = 0.034g

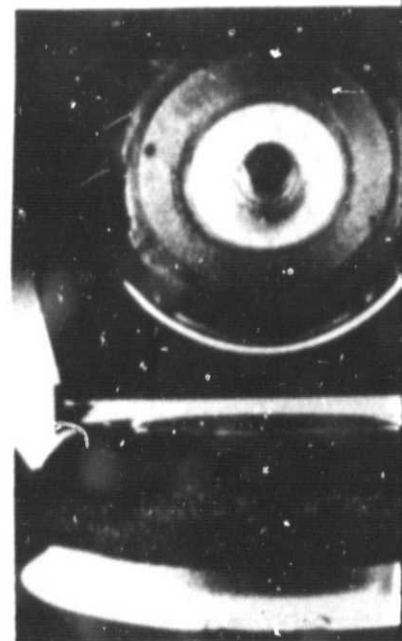(c)   Time = 0.5 Sec.
Axial Acceleration = 0.034g
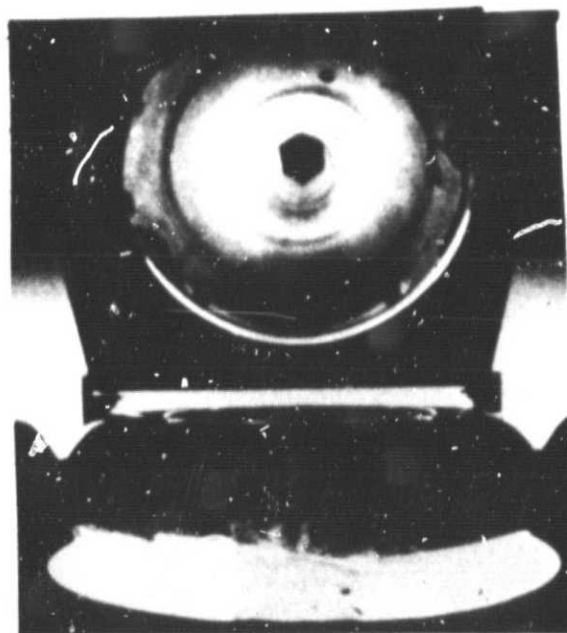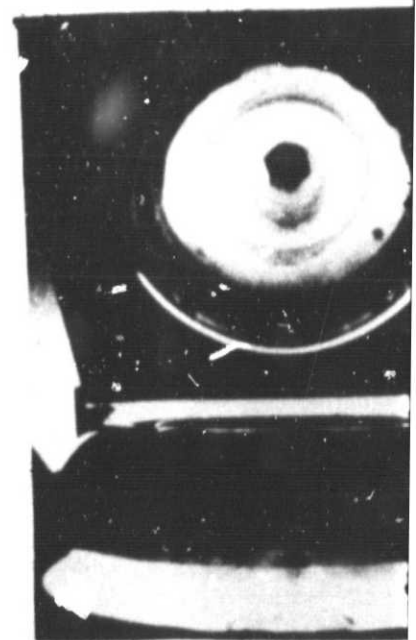

Time = 1.5 Sec.
Axial Acceleration = 0.034g

(f)   Time = 2.0 Sec.
Axial Acceleration = 0.034g
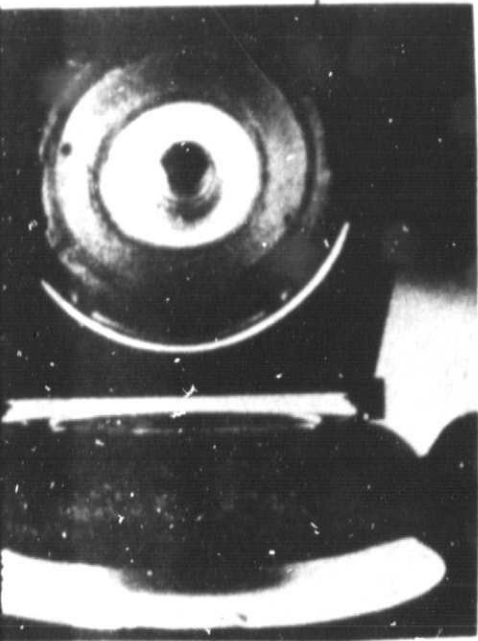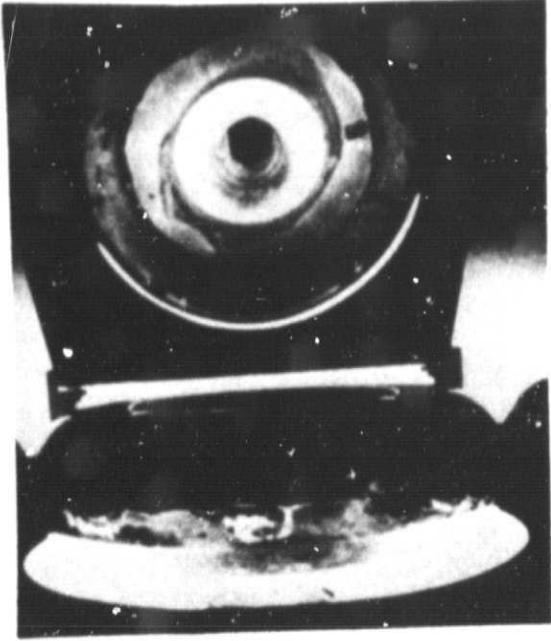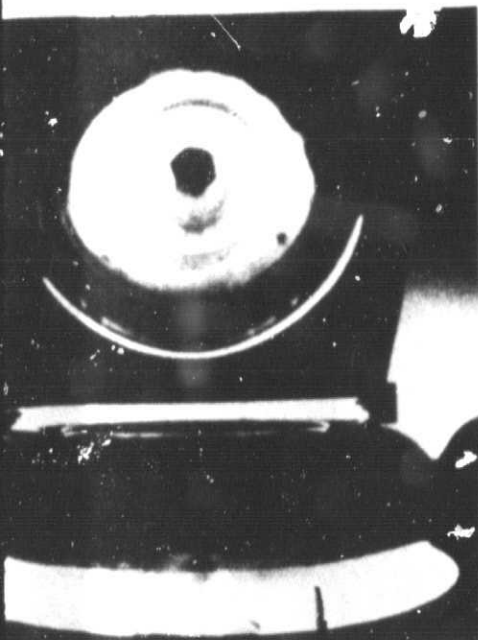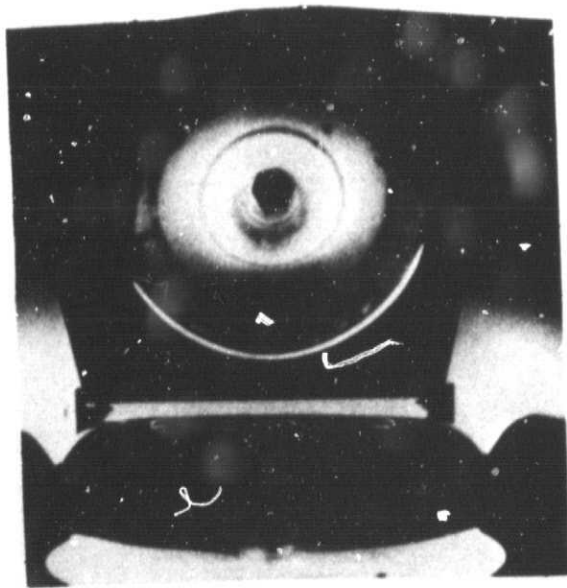
uid Settling Test with a Propellant Acquisition Device
quid Volume = 50%, Spin-Rate = 20 rpm)

tank surfaces because of the high radial acceleration associated with the 50-rpm spin rate. This radial acceleration is approximately 5 times greater than the 0.034g axial acceleration. After approximately 1.9 seconds, the liquid appeared uniformly distributed on the outer tank wall. No direct contact existed between the liquid bulk and the acquisition device retaining ring. However, the liquid was in contact with the four feeder arms.

For the testing of the 50% liquid volume at 15 and 25 rpm spin rates, the same condition existed as at 20 rpm. Specifically, there was still observed some fluid motion at the end of the drop test. While this motion did not appear to be extremely fast or violent, this condition does indicate that the largest liquid volume tested (50%) appears to present the worst case as far as liquid settling and slosh is concerned. Some additional baffling may be desired to retard or damp the motion completely.

C.   SPACECRAFT WOBBLE EFFECTS

The third type of tests performed during the test program was evaluation of the effects of spacecraft wobble on the fluid behavior in the toroidal tank. Spacecraft wobble in a spinning spacecraft may be caused by a misalignment of the engine thrust vector with the spacecraft spin axis or a misalignment of the spacecraft spin axis and longitudinal axis owing to migration of the center-of-mass. Spacecraft wobble could induce propellant perturbations or sloshing that might impose unduly large requirements upon the spacecraft attitude-control system. The purpose of these tests was to investigate propellant orientation and stability in the spinning torus when subjected to simulated spacecraft wobble. Both bench and drop tower tests were used.

Bench testing was performed first with a liquid volume of 75%, using methanol as the test fluid. The testing was accomplished using both the flexible and solid bent shafts, previously discussed. The first tests performed with the flexible shaft consisted of forcing the shaft against its 2° stop while the tank was spinning and then releasing. The objective was to determine if fluid oscillations induced when the shaft was released would be magnified or damped out. Spin rates of 50 and 100 rpm were used. The second type of bench test with the flexible shaft involved manually cycling the tank spin rate from an initial steady value to zero and back to the initial value. Reducing the spin rate to zero would induce a wave pattern on the liquid-gas interface. Returning the spin rate to its initial value would either magnify or damp out the wave pattern. Initial spin rates of 50, 100, and 150 rpm were employed.

Two types of tests were also performed with the solid, bent shaft. First, observations of fluid behavior were made with the tank rotating at constant rates of 50 and 100 rpm. Then, the manually cycled spin rate procedure described for the flexible shaft tests was also applied to the solid, bent shaft. Initial spin rates of 50, 100, and 150 rpm were employed.

Drop tower testing was also employed in the analysis of wobble effects using water as a test fluid. The change of test fluid was required when it was found that methanol attacked the cement used to bond the two halves of the tank together over a period of time. For the qualitative results to be expected, water was considered an acceptable fluid. Three tests using the solid, bent shaft were performed using liquid volumes of 75, 50, and 25%. A fourth drop test using the flexible shaft and a liquid volume of 75% was also performed. All drop tests were performed under zero-g axial acceleration and a radial acceleration of 0.06g. This radial acceleration corresponds to that experienced in the full-size propellant tank and is obtained with a spin rate of 30 rpm in the test tank.

Results of the bench tests employing the flexible shaft are given in the next two figures. Figure 20 shows the orientation of the liquid at two times during the test employing the 50-rpm spin rate. The diamond-shaped marker is attached to the tank for reference purposes. Figure 20(a) shows the conditions just after the spin axis had been released from its 2° maximum displacement. The small bent rod shown was used to displace and hold the spin axis against its stop while spinning prior to starting the test. In Figure 20(a), the tank has moved as a result of the flexible coupling spring action toward the right so that liquid is seen to be accumulating on the left side of the tank. At this time, some oscillations were also generated on the surface of the liquid. After approximately 3.0 seconds, these oscillations were damped with the fluid uniformly distributed about the spin axis as shown in Figure 20(b). A second test employing a spin rate of 100 rpm produced the same results as the 50 rpm test except that the initial oscillations appeared to be damped sooner, approximately 2.0 seconds after release. The reduced damping time is attributed to the higher radial acceleration associated with the 100 rpm spin rate.

Typical results of bench tests conducted with the flexible shaft and manually cycling the initial steady spin rate, to zero and then back to the steady value, are represented by Figure 21. This particular test was for an initial spin rate of 50 rpm. In Figure 21(a), which has been designated as time zero, the
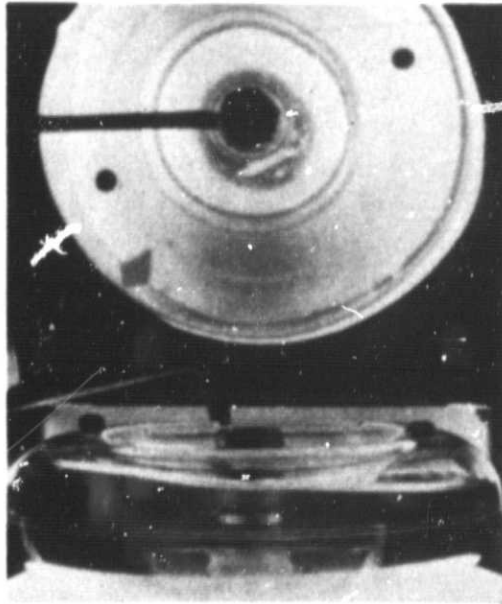
(a) Fluid Orientation After
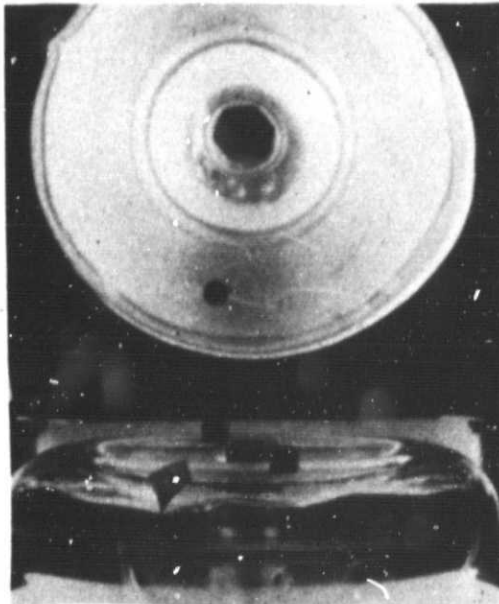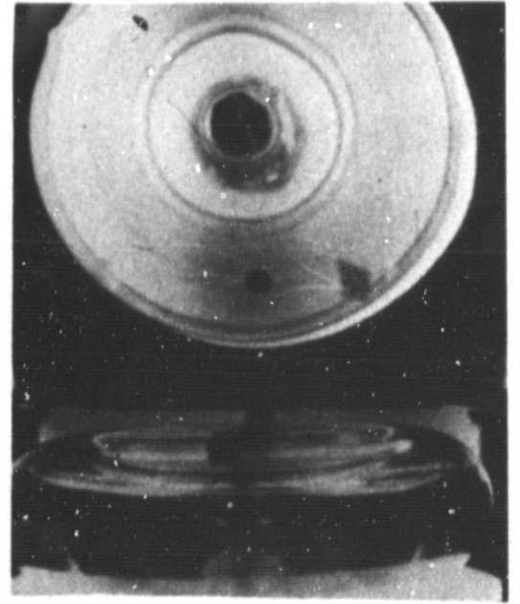   Release of Shaft
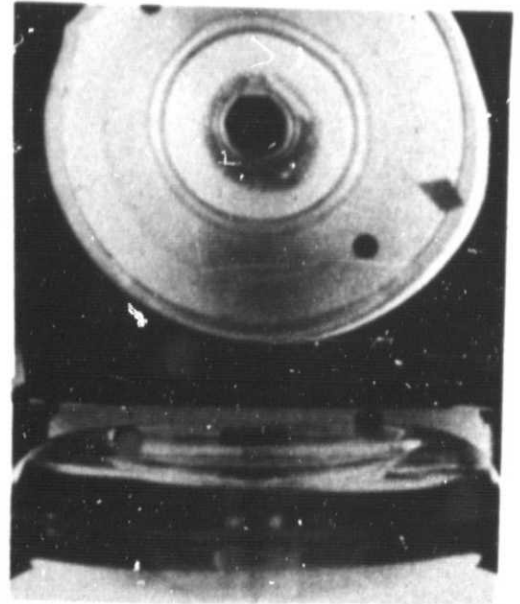
(b) Fluid Orientation After 3.2 Sec.

Figure 20: Bench Wobble Test Using Flexible Shaft
            (Liquid Volume = 75%, Spin-Rate = 50 rpm)

(a) Time = Zero Sec.
     Spin-Rate = Zero rpm
     Induced Sloshing

(b) Time = 3.2 Sec.
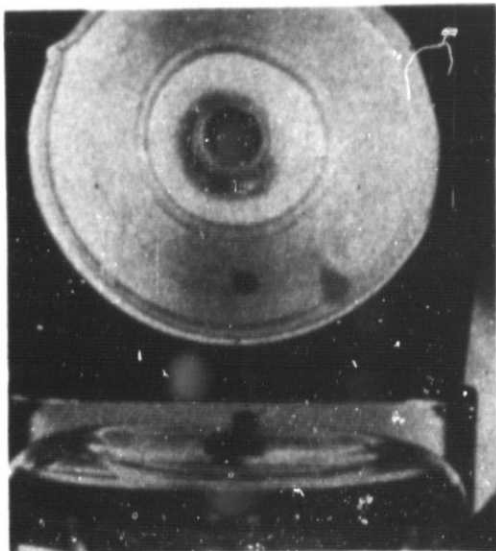   Spin-Rate = 50 rpm

Figure 21: Bench Wobble Test Using Flexible Shaft
            (Liquid Volume = 75%, Spin-Rate Cycled)

spin rate has been reduced from 50 rpm to zero and the induced sloshing is visible. In Figure 21(b), which is 3.2 seconds later, the spin rate has been returned to 50 rpm and the fluid sloshing has been damped out. Similar results are obtained with the 100 and 150 rpm spin rates except the apparent damping time was less, being approximately 2.7 and 2.8 seconds.

In the series of bench tests conducted with a solid spin shaft bent at an angle of 2°, observations of the fluid orientation in the tank under steady-state spinning at 50, 100, and 150 rpm indicated no significant oscillations or sloshing. In general, the liquid tends to accumulate in that portion of the torus farthest away from the spin axis (i.e., in the direction the shaft is bent). This is more pronounced at higher spin rates because of the higher resultant centrifugal forces. Figures 22 and 23 show the liquid orientation for spin rates of 50 and 100 rpm, respectively. In both figures, part (a) shows the shaft bent to the right while part (b) represents a 180° rotation with the shaft bent to the left. In both cases, the interface appears to be stable with no oscillations or perturbations.

Results of bench tests in which the spin rates were manually cycled were essentially the same with the solid bent shaft as those noted with the flexible shaft with one possible exception. It appeared that, with the solid bent shaft, the induced slosh was amplified significantly when the tank spin rate was increased from 0 to its initial value. This was especially evident for the 100- and 150-rpm spin rate tests. However, although the slosh problem appeared to be aggravated, the damping times did not change appreciably. After 3.4 seconds in the test at 50 rpm, the liquid-gas interface was stable and non-oscillatory. Approximately 2.8 seconds were required to reach corresponding conditions in the 100- and 150-rpm tests. Figures 24, 25, and 26 present results for the 50, 100, and 150 rpm tests, respectively.

The first drop test, using the solid shaft and 75% liquid volume, produced no large sloshing or fluid oscillations as a result of the simulated wobble. However, an unsymmetrical liquid distribution was established because of the tilted tank orientation. The liquid mass tended to move to the region of the tank farthest from the spin axis. The fluid displacement, together with a low Bond number (2.8), resulted in a corresponding displacement of the ullage bubble into a toroidal segment. This condition is shown in Figure 27 at 1.5 seconds after initiation of the drop test. At this time, the liquid-gas interface appeared to be stable and quiescent. The solid black line around the middle of the tank in Figures 27 through 30 was placed on the tank for reference purposes.
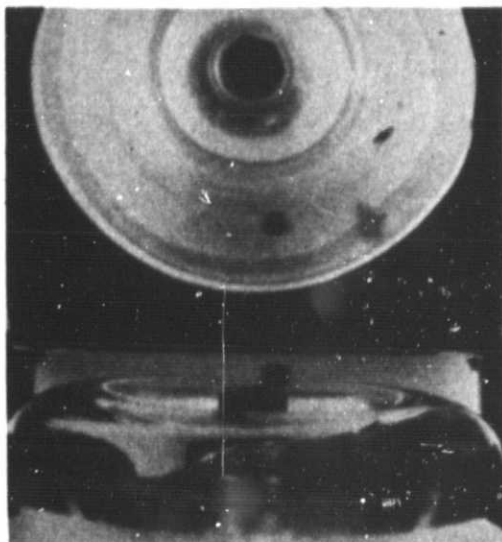
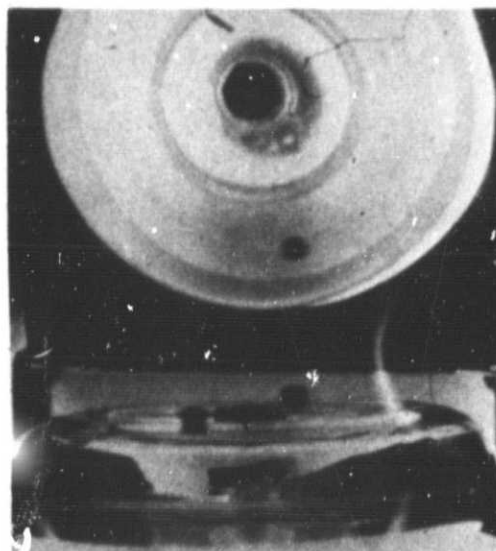(a)   Shaft Bend to the Right   (b)   Shaft Bend to the Left

Figure 22:   Bench Wobble Test Using Solid, Bent Shaft
(Liquid Volume = 75%, Spin-Rate = 50 rpm)

(a)   Shaft Bend to the Right   (b)   Shaft Bend to the Left

Figure 23:   Bench Wobble Test Using Solid, Bent Shaft
(Liquid Volume = 75%, Spin-Rate = 100 rpm)
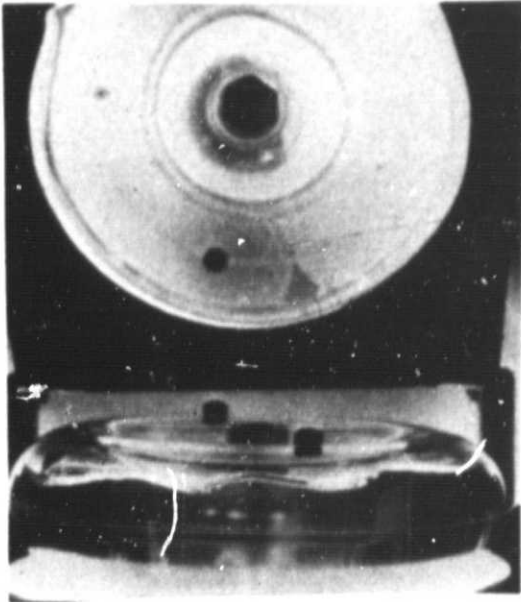
(a) Time = Zero Sec.
     Spin-Rate = Zero rpm
     Induced Sloshing
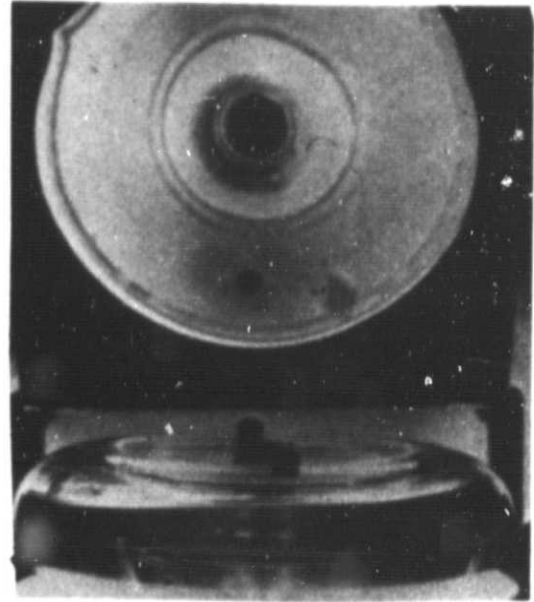
(b) Time = 3.4 Sec.
     Spin-Rate = 50 rpm

Figure 24: Bench Wobble Test Using Solid, Bent Shaft
            (Liquid Volume = 75%, Spin-Rate Cycled,
            Initial Spin-Rate = 50 rpm)

(a) Time = Zero Sec.
     Spin-Rate = Zero rpm
     Induced Sloshing

(b) Time = 2.7 Sec.
     Spin-Rate = 100 rpm

Figure 25: Bench Wobble Test Using Solid, Bent Shaft
            (Liquid Volume = 75%, Spin-Rate Cycled,
            Initial Spin-Rate = 100 rpm)

38

(a) Time = Zero Sec.
     Spin-Rate = Zero rpm
     Induced Sloshing

(b) Time = 2.8 Sec.
     Spin-Rate = 150 rpm

Figure 26: Bench Wobble Test Using Solid, Bent Shaft
            (Liquid Volume = 75%, Spin-Rate Cycled,
            Initial Spin-Rate = 150 rpm)

Figure 27: Drop Tower Wobble Test Using Solid, Bent Shaft
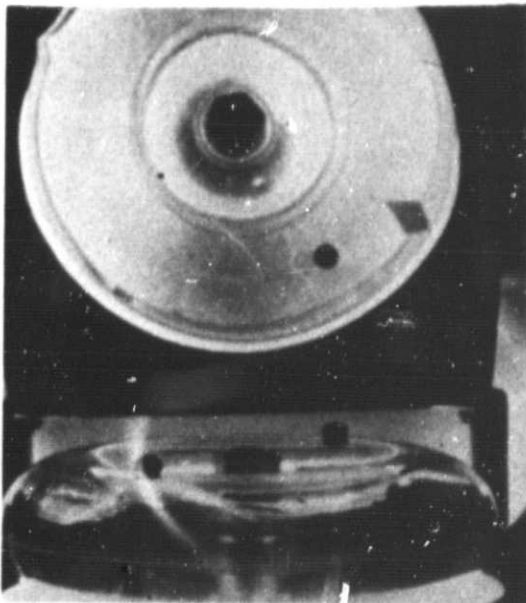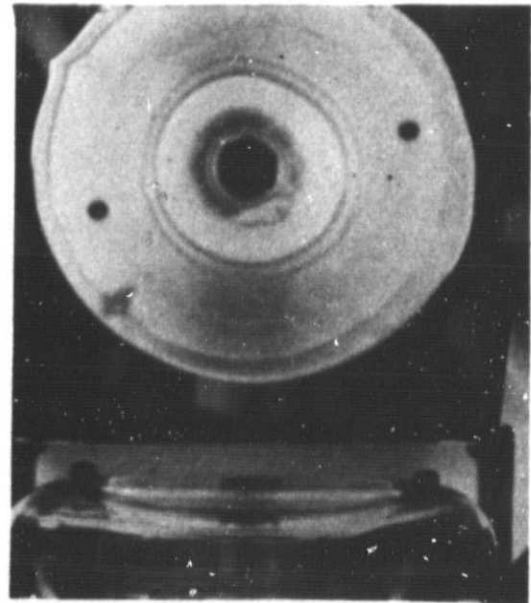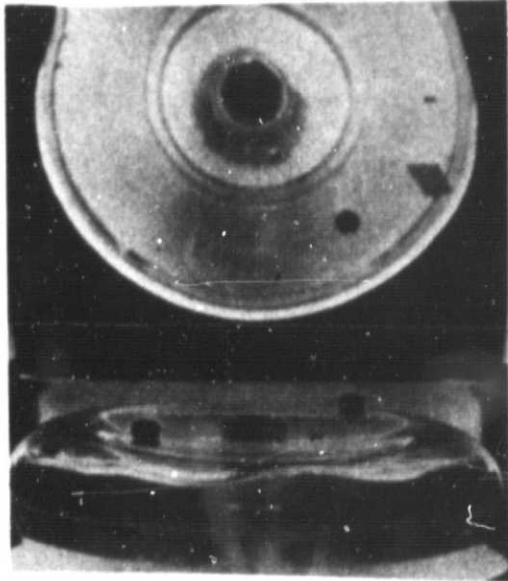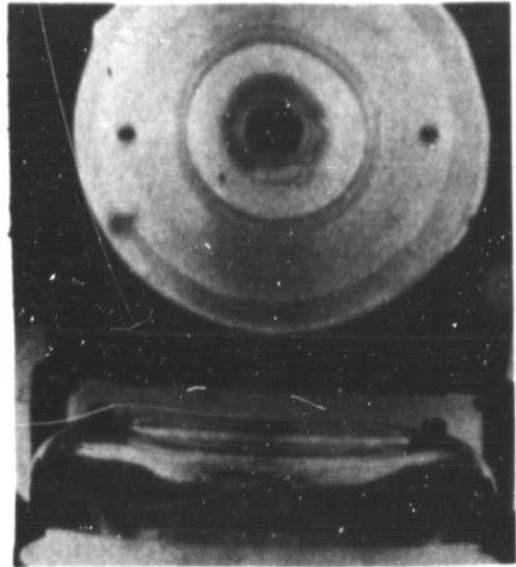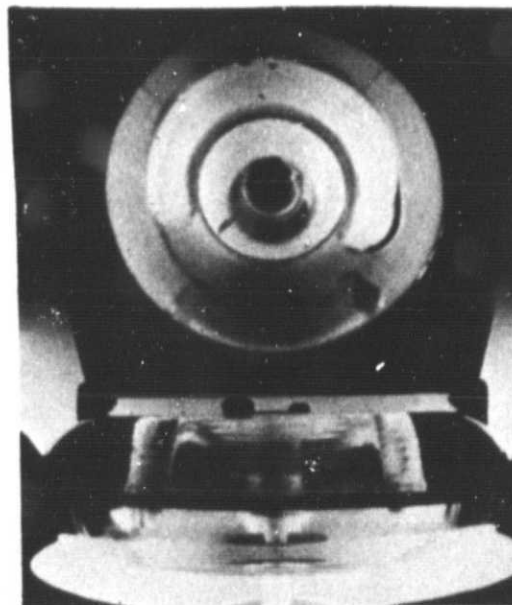   (Liquid Volume = 75%, Spin-Rate = 30 rpm,
            Time = 1.5 Sec.)

In the second drop test with the solid shaft and a liquid volume of 50%, no ullage breakup was observed although the liquid was distributed unsymmetrically. The test results at 1.5 seconds are shown in Figure 28. No significant oscillations of the liquid-gas interface were observed.

For the third test with 25% liquid volume, significant fluid displacement was noted. Figure 29, taken at 1.5 seconds during the test, shows that the liquid is concentrated on the left side of the tank in the direction of the bent shaft. At this time, definite fluid motion was still observed in the drop-test film. This motion was not rapid or oscillatory in nature but did continue until the end of the test. Thus liquid settling, as observed in the two previous tests, had not been accomplished at the end of the drop test for this volume. Wobble effects appear to influence fluid behavior more at smaller liquid volumes.

In the fourth drop test with the flexible shaft and a liquid volume of 75%, some fluid oscillations were observed at the start of the drop during reorientation from a normal one-g environment to a near-zero-g condition. However, these oscillations were soon damped out and a stable, uniform liquid-gas interface was observed. Figure 30 illustrates the fluid distribution at 1.5 seconds. The fluid oscillations did not impose sufficient forces on the rotating tank wall to displace the tank against the 2° stop on the flexible shaft.

D.   SPACECRAFT SPIN RATE CHANGE EFFECTS

The spacecraft spin rates during cruise modes or during imaging at the planet are relatively low. However, when major velocity changes are made, higher spacecraft spin rates are required to minimize the effects of thrust misalignments. A major concern is that changing the spin rate might induce propellant sloshing or displacement that could affect spacecraft attitude and control. The objective of the spin rate change tests was to investigate propellant orientation and behavior in the toroidal tank when the spin rate was changed. A minimum spin rate change of 1 rpm/sec was to be simulated. All spin rate change tests were performed in the drop tower with zero-g axial acceleration. During the drop test, a ramp change in voltage to the drive motor was applied during the 2.1 sec test. This voltage produced a linear change in spin rate during the drop.

Test conditions for the model tank were based on tangential velocities and accelerations to be expected with the full-size tank. For the model tank, an initial spin rate of 50 rpm and a
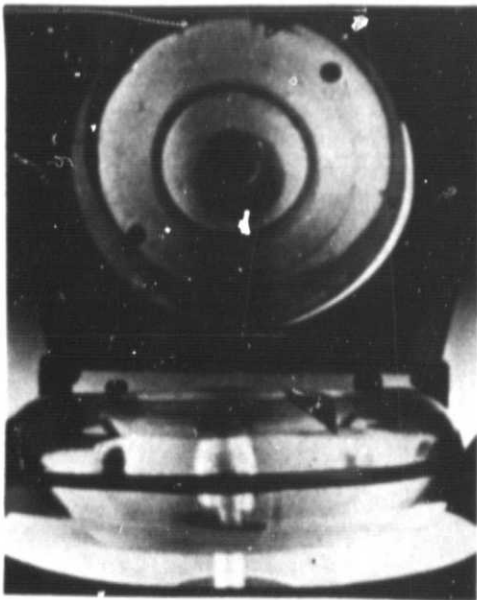
Figure 28: Drop Tower Wobble Test Using Solid, Bent Shaft (Liquid Volume = 50%, Spin-Rate = 30 rpm, Time = 1.5 Sec.)
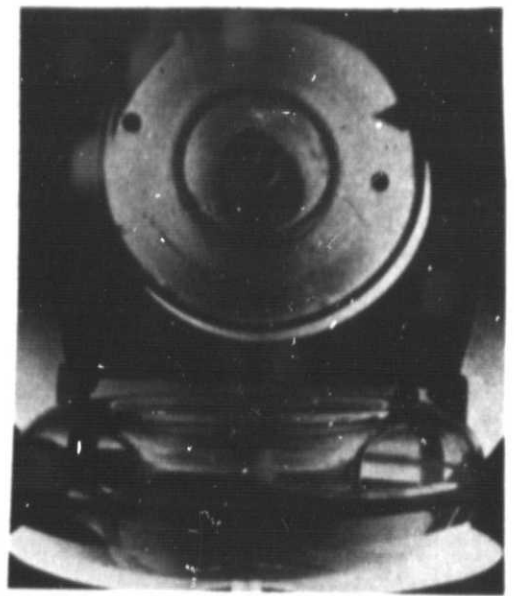

Figure 29: Drop Tower Wobble Test Using Solid, Bent Shaft (Liquid Volume = 25%, Spin-Rate = 30 rpm, Time = 1.5 Sec.)
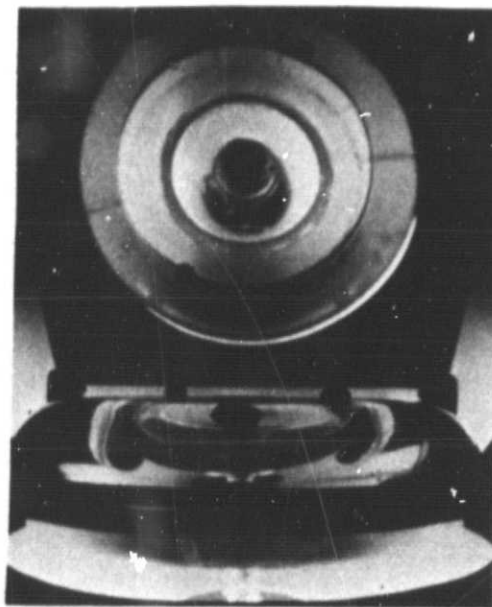

Figure 30: Drop Tower Wobble Test Using Flexible Shaft (Liquid Volume = 75%, Spin-Rate = 30 rpm, Time = 1.5 Sec.)

spin-rate change of 10 rpm/sec would be approximately equivalent
to 5 rpm and 1 rpm/sec in the full-size tank. These conditions
were taken as a baseline.

Additional testing at a higher spin-rate change and a higher
initial spin rate was performed. A total of four tests were
completed as follows:

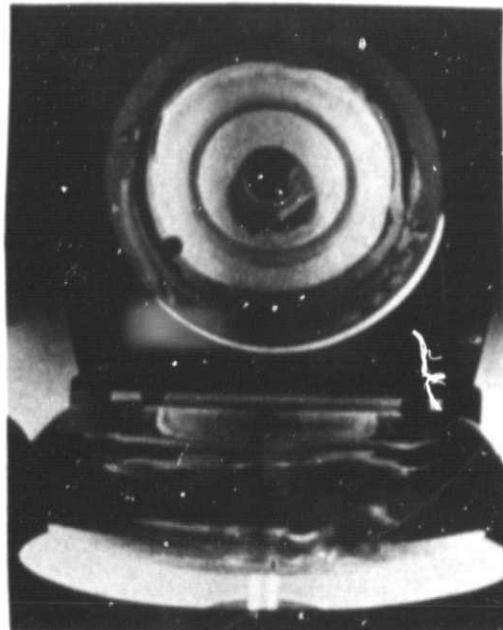| Initial Spin Rate, rpm	Spin Rate Change, rpm/sec
50	10
50	40
100	10
100	40

The test fluid used was methanol.

The first test, conducted with an initial spin rate of 50 rpm
and a spin-rate change of 10 rpm/sec, approximately simulates
conditions specified for the full-size tank described in Ref-
erence 1. Figure 31 presents a time series of photographs from
this test. In Figure 31(a), the initial orientation of the liquid
is presented. · the start of the drop, the spin-rate change of
10 rpm/sec is applied to the tank. Figures 31(b), (c), and (d),
illustrate fluid orientation in the tank at 0.5, 1.0, and 1.8
seconds, respectively. In general, the liquid-gas interface is
oriented parallel to the tank spin axis. Some oscillations and
fluid motion are visible in both the top and front view of the
tank. Part of this motion resulted from the transition from a
one-g to a zero-g environment at the start of the drop test.
Thus, the sloshing motion observed is more severe than would
actually be expected. At any rate, the observed sloshing did
not appear to amplify as time progressed.

Results of the second test with the spin-rate change of 40 rpm/
sec are similar to the first test except that more turbulence is
noted, both on the liquid-gas interface and within the liquid.
This is to be expected since the higher spin acceleration will
induce larger tank wall tangential velocities in the same period
of time. Figure 32 shows the liquid orientation at 1.6 seconds
after the start of the drop test. Comparison of this figure with
Figure 31(d) (for 10 rpm/sec) will illustrate the difference noted.

Results of doubling the initial spin rate are shown in Figures 33
and 34. Again, increasing the spin acceleration from 10 rpm/sec
(Figure 33) to 40 rpm/sec (Figure 34) increases the degree of
turbulence as anticipated. If Figure 33 is compared with
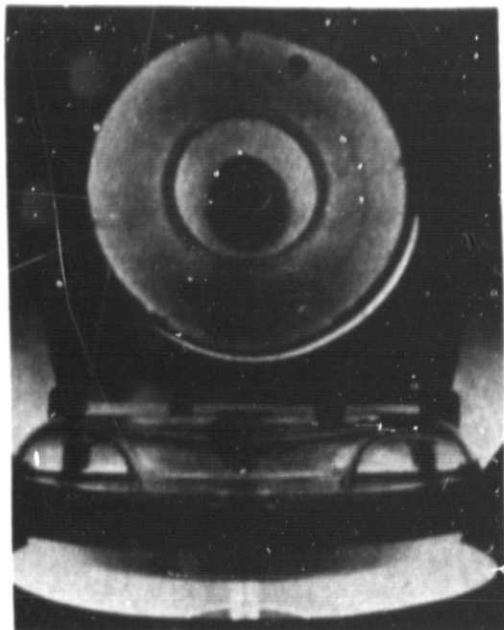
(a) Time = Zero Sec.
     Spin-Rate = 50 rpm

(b) Time = 0.5 Sec.
     Spin-Rate = 55 rpm
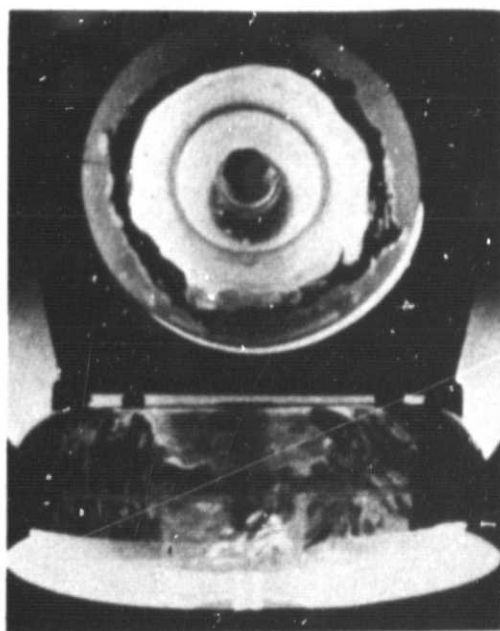
(c) Time = 1.0 Sec.
     Spin-Rate = 60 rpm
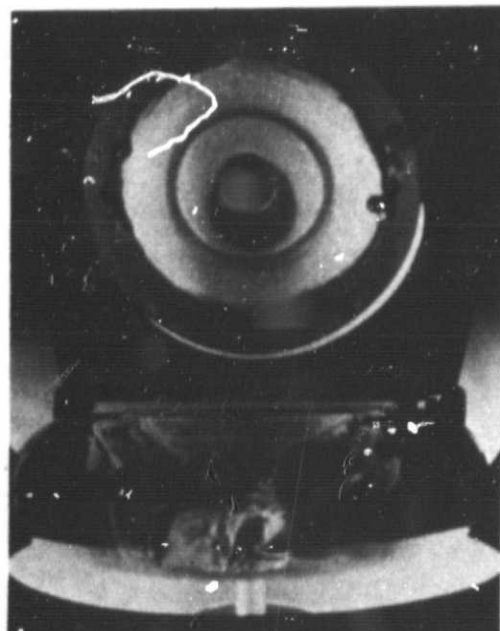
(d) Time = 1.8 Sec.
     Spin-Rate = 68 rpm

Figure 31: Spin-Rate Change Eff cts Test (Liquid Volume = 50%, Initial
            Spin-Rate = 50 rpm, Spin-Rate Change = 10 rpm/sec.)

43
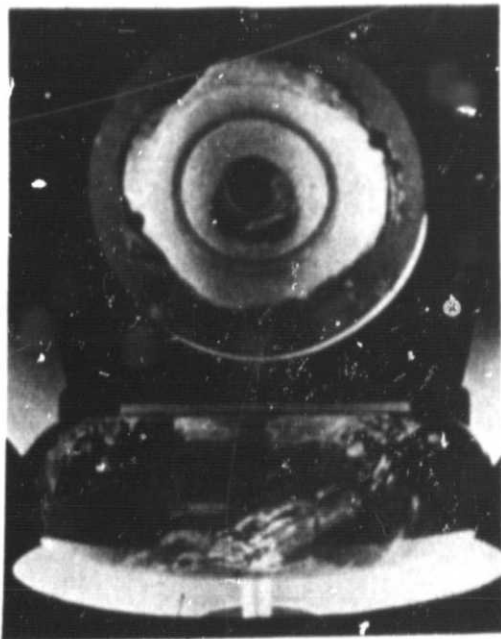
Figure 32: Spin-Rate Change Effects Test (Liquid Volume = 50%, Initial Spin-Rate = 50 rpm, Spin-Rate Change = 40 rpm/sec, Time = 1.6 Sec.)
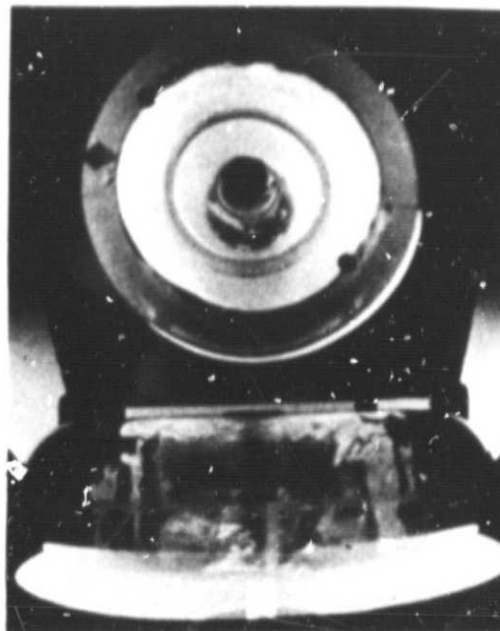
Figure 33: Spin-Rate Change Effects Test (Liquid Volume = 50%, Initial Spin-Rate = 100 rpm, Spin-Rate Change = 10 rpm/sec, Time = 1.5 Sec.)
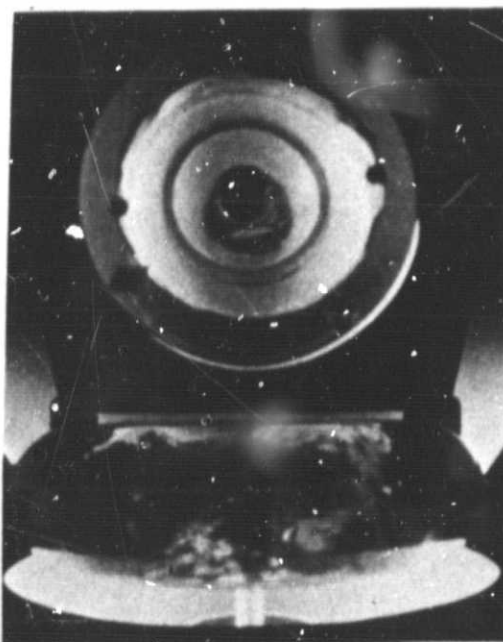
Figure 34: Spin-Rate Change Effects Test (Liquid Volume = 50%, Initial Spin-Rate = 100 rpm, Spin-Rate Change = 40 rpm/sec, Time = 1.5 Sec.)

44

Figure 31(d), it also appears that, for the same spin-rate
change, the higher initial spin rate will produce a smoother,
less turbulent interface.

The discussions of the test results presented in the previous
sections have been primarily concerned with the effects as ob-
served in the scale model tank. In this section, the relation
of these observed results to the fluid behavior expected in the
full-size tank are briefly analyzed.

Results of the ullage-orientation tests are believed to be
directly applicable to any of the four specified propellants
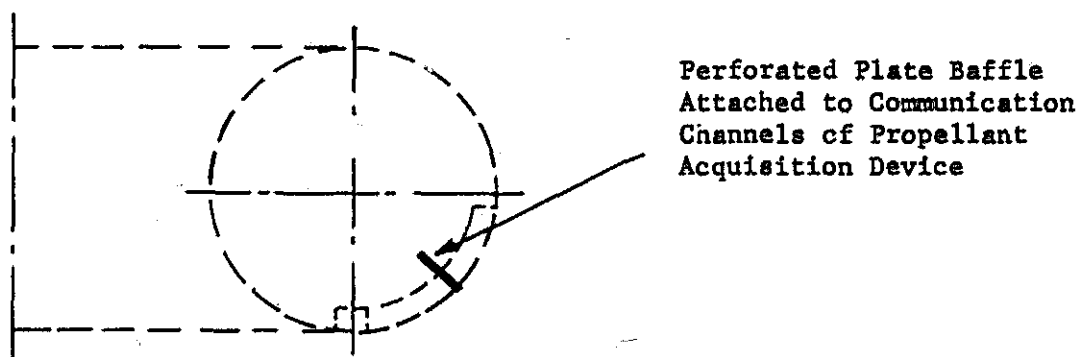in the full-size tank (or larger) at a spin rate of 10 rpm (or
higher), since the test Bond number was equal to or less than
those of the four propellants. Hence, in the absence of perturb-
ing forces, the propellants simulated in these tests can be ex-
pected to be symmetrically distributed about the spin axis prior
to engine ignition.

The liquid settling tests performed with the scale-model tank
are considered conservative since the transition from one-g to
low-g and the location of the test fluid at the top of the tank
combine to induce more severe initial sloshing than would be
expected in the full-size tank in which the acceleration changes
from zero-g to low-g and the propellants are distributed sym-
metrically along the outer tank wall. On the basis of the ob-
servations, no major sloshing conditions are anticipated in the
full-size tank. Additional baffling could be easily incorporated
if desired for fluid volumes greater than 25%. Two possible low
weight baffling arrangements are shown in Figure 35. In Figure
35(a), a baffle made from perforated plate is attached to the
inner torus wall, as shown. As liquid moves down the outer wall
and over the retaining ring in the bottom of the tank, it will
impact on the vane on the inner tank wall losing some or all of
its kinetic energy. Axial and radial accelerations would then
tend to return the liquid to the vicinity of the retaining ring.
The second baffling arrangement would consist of a perforated
plate extending between the communication channels, as shown in
Figure 35(b). With this baffle, the liquid velocity would be
reduced before the liquid reached the retaining ring. There are
other possible baffling arrangements including a combination of
the two just discussed. More analytical and experimental work
would be required to define suitable configurations and dimensions.

The maximum liquid volume considered in the liquid settling test
was 50% based on information from Reference 4, that this volume
in spheres was the worst case for slosh. However, disturbing
forces and moments in the toroidal tank may be larger at liquid

Perforated Plate Baffle
Attached to Inner Tank
Wall

(a) Inner Baffle
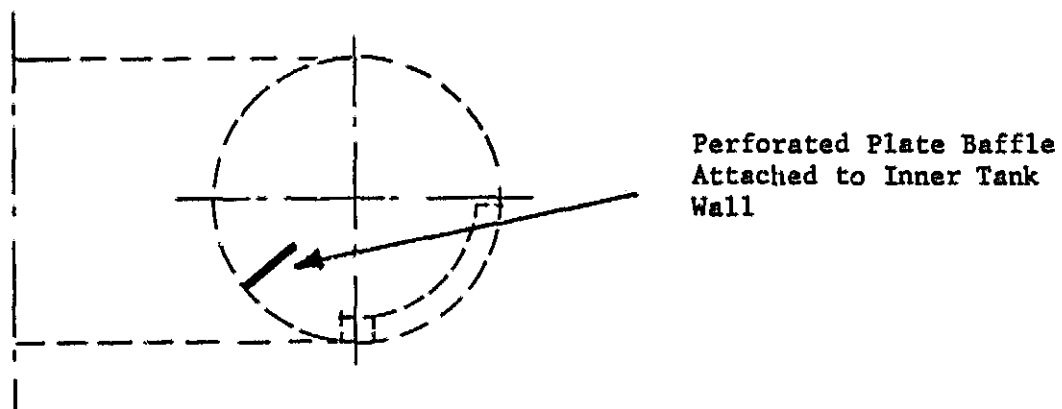
Perforated Plate Baffle
Attached to Communication
Channels of Propellant
Acquisition Device

(b) Baffle Between Communication Channels

Figure 35: Possible Slosh Baffling Arrangements

volumes above 50% because of greater masses of liquid in motion. Additional testing of the toroidal tank at larger liquid volumes would be necessary to verify this assumption.

The spacecraft wobble tests performed with the bench facility indicated no significant sloshing problems would be experienced in the full-size tank as a result of wobble. Artificially gen- erated wave motions were damped rather than amplified by the tank spin rate. The drop tests, however, indicated that an unsym- metrical propellant distribution can result from wobble in the full-size tanks. Two factors were involved in these tests. First, the solid, bent shaft used to simulate wobble motion of the spacecraft caused an unsymmetrical distribution of the liquid about the spin axis. Secondly, the spin rate used in the test produced a low Bond number of 2.8. For the test with the tank 75% full, these two factors combined to result in a displaced ullage bubble in the shape of a toroidal segment. For the 50% volume tests, the ullage was stable (no breakup) but the liquid was unsymmetrically distributed. For the 25% test, the liquid mass was essentially concentrated on one side of the tank. The spacecraft in which the full-size tanks might be used is currently designed to provide for damping of this wobble motion with four spherical tanks. The substitution of two toroidal tanks can be expected to impose requirements for such damping no greater than, and probably less than, those currently provided. Depending on the frequency of the propellant motion in the spinning toroidal tanks, the wobble damping requirements could be reduced by pro- pellant viscous effects.

Results of the spin-rate change tests indicate that, for spin accelerations representative of the spacecraft, no major slosh problems are anticipated during spin-up and spin-down with the present propellant acquisition system design. However, addition of baffling to this design for liquid settling, as discussed earlier, might result in fluid motions during spin-rate changes which could disturb the spacecraft attitude. In this case, a smaller spin acceleration might be employed.

A.   CONCLUSIONS

In general, no major fluid behavior problems were identified
during testing of a spinning toroidal tank under both bench and
drop tower tests. Specific conclusions reache. were as follows:

1)   In the absence of perturbing forces during coast under
      zero-g conditions, propellant distribution should be uniform
      and the ullage should be stable and symmetrical in the tank
      because of the spacecraft spin stabilization. No breakup
      of the ullage bubble should occur for any of the specified
      propellants.

2)   No major slosh problems are expected during liquid settling.
      Additional baffling can be easily incorporated, if desired,
      for liquid volumes in excess of 25%.

3)   Additional experimental work is required to establish natural
      frequency and slosh force data in spinning toroidal tanks
      because this information does not appear to be readily
      available.

4)   Unsymmetrical distribution of propellant resulting from space-
      craft wobble appears to be the most critical fluid behavior
      problem in the spinning toroidal tank. However, this problem
      is not considered serious since the proposed spacecraft with
      four spherical tanks is provided with a damper to reduce
      wobble to zero and replacement of the spheres with two tor-
      oids is not expected to increase the damping requirements.
      In fact, a reduction in damping requirements may occur as a
      result of propellant viscous effects.

5)   During spin rate change tests, the liquid-gas interface was
      oriented essentially parallel to the spin axis. Fluid oscil-
      lations and perturbations on the interface were distributed
      fairly uniformly around the surface. No definite amplifi-
      cation of these oscillations was apparent. Therefore,
      changing the spacecraft spin rate did not produce signifi-
      cant sloshing motion.

B.   RECOMMENDATIONS

As a result of the findings during the feasibility study preceding this test program and the observations obtained from these tests, the following recommendations are made for future toroidal tank development.

1) Slosh tests should be performed on subscale models to determine natural frequencies, forces, and damping factors in a spinning toroidal tank. Tests should be performed with and without propellant acquisition devices.

2) Outflow tests of a subscale model should be performed under one-g conditions to verify design of the propellant acquisition device. Both static and spinning conditions would be demonstrated.

3) Additional drop tower tests should be performed to further investigate spacecraft wobble effects. The test tank would be driven by a flexible coupling which would allow the tank to wobble while spinning.

4) Additional drop tests should be performed to determine lower Bond number limit for ullage breakup as a function of liquid volume.

5) A full-size propellant tank and acquisition device should be fabricated and assembled to demonstrate the ability to manufacture these systems. Subsequent to manufacture, the tank would be subjected to fluid behavior tests such as slosh, fill and drain, and outflow.

REFERENCES

HTS-73-1903

1. John E. Anderson and Dale Fester: A Feasibility Study of
   Developing Toroidal Tanks for a Spinning Spacecraft. MCR-
   73-223. Martin Marietta Corporation, Denver, Colorado,
   September 1973 (Contract NAS2-7489).

2. Study of Alternate Retro-Propulsion Stage Configurations for
   the Pioneer Outer Planet Orbiter. 22303-6003-RU00. TRW
   Systems Group, Redondo Beach, California, November 30, 1973
   (Contract NAS2-6859).

3. H. L. Paynter: Time for a Totally Wetting Liquid to Deform
   From a Gravity-Dominated to a Nulled-Gravity Equilibrium
   State. AIAA J. Vol. 2, No. 9, September 1964, p 1627.

4. H. N. Abramson, Ed.: The Dynamic Behavior of Liquids in
   Moving Containers. NASA SP-106. Southwest Research Insti-
   tute, San Antonio, Texas, 1966 (Contract NASr-94(07)).

5. E. P. Symons and K. L. Abdulla: Liquid-Vapor Interface
   Configurations in Toroidal Tanks During Weightlessness.
   NASA TND-4819. Lewis Research Center, Cleveland, Ohio,
   October 1968.

6. E. P. Symons: Zero Gravity Equilibrium Configuration of
   Liquid-Vapor Interface in Toroidal Tanks. NASA TND-6076.
   Lewis Research Center, Cleveland, Ohio, November, 1970.

7. L. J. Hastings and R. Rutherford: Low Gravity Liquid-
   Vapor Interface Shapes in Axisymmetric Containers and a
   Computer Solution. NASA TMX-53790. George C. Marshall
   Space Flight Center, Huntsville, Alabama, October 7, 1968.

8. J. L. McCarty, et al.: Experimental Investigation of the
   Natural Frequencies of Liquids in Toroidal Tanks. NASA
   TND-531. Langley Research Center, Langley Field, Virginia,
   October 1960.